IEEE Access
Multidisciplinary | Rapid Review | Open Access Journal

Received July 18, 2021, accepted July 27, 2021, date of publication July 30, 2021, date of current version August 10, 2021.

Digital Object Identifier 10.1109/ACCESS.2021.3101463

An Average Voltage Approach to Control Energy Storage Device and Tap Changing Transformers Under High Distributed Generation

NDAMULELO TSHIVHASE[1], ALI N. HASAN[2], AND THOKOZANI SHONGWE[1], (Member, IEEE)
[1]Department of Electrical and Electronic Engineering, University of Johannesburg, Johannesburg 2006, South Africa
[2]Department of Electrical Engineering, Higher Colleges of Technology, Abu Dhabi, United Arab Emirates

Corresponding author: Ndamulelo Tshivhase (200831989@student.uj.ac.za)

ABSTRACT The South African power distribution network is characterized by long power distribution lines with low short circuit capacity, and when distributed generation is introduced to these lines, voltage magnitudes are severely impacted. The existing voltage regulation methods of the on-load tap changer and step voltage regulator cannot successfully regulate voltage in long distribution lines with distributed generation since their control philosophy was designed for networks without distributed generation. Therefore, a dynamic system is proposed in this paper that coordinates the on-load tap changer, step voltage regulator, distributed generators, and the battery energy storage system to control voltage in long distribution lines with distributed generation. Their coordination will be based on response time and robustness. Unlike the conventional method, the proposed novel system will calculate a reference voltage that the on-load tap changer and the step voltage regulator must follow, based on the real time average voltage of the section of the network they each regulate. The system will also control the charging and discharging of a battery energy storage system based on the point of connection voltage and the average voltage of the feeder which it is connected to. Reactive power from distributed generators will also be used to enhance voltage regulation and refine the network power factor. When voltage magnitudes cannot be successfully brought within acceptable range, the proposed scheme will decrease the active power produced by distributed generators. The proposed system is examined on a South African 22kV network built in Matlab/Simulink.

INDEX TERMS Active distribution system, Active power, battery energy storage system, distributed generator, on-load tap changer, reactive power, step voltage regulator, voltage regulation.

I. INTRODUCTION

Renewable energy sources have gained more attention in the last decade. This increased attention is motivated by the pollution associated with conventional coal fired power generating stations. Most of these renewable energy sources are small scale and distributed throughout the power system, hence, they are also called distributed generators (DGs). However, the connection of these DGs to the power distribution network introduces operational challenges [1]. The major challenge introduced is voltage regulation, when DGs export active power during low loading conditions, the voltage magnitude where they are connected can rise above the power utility's prescribed voltage limits [1]–[4]. The rise in voltage magnitude will be worse when the DG is connected to a low short circuit capacity network, also referred to as a weak network [5]–[7]. The South African power distribution network is characterized by long power distribution lines, some of these lines spanning between fifty and a hundred kilometres. The high impedance towards the end of such long distribution networks, and the resulting low short circuit capacity make them weak networks, where the voltage is extremely sensitive to both active and reactive power [8]. Therefore, when DGs are introduced in such weak locations of the power distribution network, their impact on voltage is extremely high. However, these long distribution networks have voltage regulation techniques that they use to keep voltage magnitudes well-regulated, which include the on-load tap changer (OLTC) and the step voltage regulator (SVR). The OLTC is situated at the main substation and regulate voltage by ensuring that

The associate editor coordinating the review of this manuscript and approving it for publication was Bin Zhou.

a predetermined and fixed voltage magnitude is kept at its secondary busbar [9]. Since the peak load and impedance of a power distribution feeder are known, and the voltage drop at the furthest point can be estimated, the OLTC fixed reference voltage is determined such that the furthest point in all feeders is above minimum acceptable voltage during peak loading conditions [10]. However, for long power distribution feeders, the voltage drop at the furthest point is so high such that no possible OLTC fixed reference voltage can prevent the voltage from dropping below minimum acceptable voltage. Therefore, in such long feeders, SVRs are installed along the feeders to help boost voltage magnitudes. The philosophy of operation of an SVR is similar to that of an OLTC, it keeps the voltage magnitude of interest at a predetermined and fixed voltage magnitude [11], [12]. This voltage magnitude of interest can be the voltage where it is located, or the voltage at a remote location that is estimated through the line drop compensation (LDC) technique [12]. This conventional procedure of employing both the OLTC and SVR to regulate voltage in accordance with a fixed reference voltage works in passive power distribution networks, where there are no DGs, power flows in one direction, the network load and impedance are well understood, and the voltage drop can be easily predicted. The active power distribution network that result from DG connection has power that can flow in any direction and will also experience both voltage drops and voltage rises depending on the balance between DG generation and network load.

Therefore, the OLTC and SVR static voltage regulation philosophy that relies on predictability and fixed variables cannot suffice in a network with high distributed generation. This paper will consequently introduce an innovative dynamic algorithm that enhances voltage regulation in active distribution systems with high distributed generation. The dynamic algorithm will coordinate the operation of the OLTC and SVR, and further calculate the appropriate reference voltages that each one should follow. It will further utilize a battery energy storage system (BESS) to enhance voltage regulation and reduce the number of tap operations on both the OLTC and SVR. DGs also have voltage regulation ability through the usage of reactive power, however, literature has highlighted the impact that the exchange of reactive power between the network and DGs have on the electrical network power factor [13]–[15]. Therefore, the proposed scheme will also utilize DGs reactive power to further assist in enhancing voltage regulation and boosting power factor. The proposed control system's dynamic characteristic arises from its ability to compute the setpoints of all devices it controls in real time based on real time voltage magnitudes. This is an improvement from the existing conventional system that uses fixed setpoints, and hence static.

II. LITERATURE REVIEW

Literature has explored and proposed multiple techniques that enhance voltage regulation in active power distribution networks and also use a BESS for efficient power system operation. In [14], a technique is proposed that coordinates multiple DGs to control voltage and refine the power factor. In [16], another technique is proposed that controls voltage and reduce power losses using reactive power from DGs. The technique also ensures that the reactive power is evenly distributed through all DGs. However, since DGs are being connected to a power system with existing voltage regulation devices, DGs voltage control capabilities must be coordinated with existing devices for optimal voltage regulation. By not coordinating DGs and existing voltage regulation devices, strategies in [14] and [16] will lead to conflict between devices, and the overutilization/underutilization of some devices. In [17], a technique is proposed that uses a BESS in a low voltage active distribution network to control voltage. The BESS is connected on the same bus as the DG, and its charging and discharging cycles are triggered by the amount of generated active power and the DG point of connection (POC) voltage. In [18], a technique is designed to coordinate a BESS and an OLTC for effective voltage regulation and prevent the overutilization of the BESS. The BESS regulates voltage based on its POC voltage, whereas the OLTC regulates voltage based on estimated bus voltages, BESS state of charge (SOC), and the apparent power flowing through the network. In [19], a technique is proposed to coordinate BESS, DGs and soft open points devices for optimal usage of all devices in voltage regulation.

In [20], a technique is presented that uses a BESS to reduce voltage and frequency deviation. The strategy uses multiple BESS connected at different locations, the controller then controls the charging and discharging of each BESS to control voltage and frequency in relation to the sensitivity coefficient of the BESS location and the BESS SOC. In [21], a technique is proposed that uses a BESS to ensure that wind power plants meet their frequency response obligations. The strategy considers the BESS SOC and the BESS rate of charge/discharge in operation. In [22], a technique is proposed that allows a high power generation by photovoltaic plants in a low voltage power distribution network by using a BESS to prevent overvoltage. In [23], a technique is presented that coordinate the OLTC, BESS and DGs for voltage regulation improvement. The strategy determines the optimal tap position of the OLTC at any point in time, the state of each BESS, and the reactive and active power outputs of each DG to ensure well-regulated voltage magnitudes and reduce line congestion.

In [24], a technique is proposed that coordinates a tap changing transformer with a BESS to alleviate voltage rise under high DG generation. The tap changing transformer operated using LDC where it estimates voltage at a remote bus and ensures it is equal to a fixed reference voltage. When the tap changing transformer has matched the estimated voltage with its fixed reference voltage, but other voltage magnitudes within the network are out of a defined range, the BESS will charge/discharge based on the deviation direction and the state of the network load. The state of the load will be either peak or off peak. In [25], another technique is suggested that coordinates capacitor banks, OLTC, DGs and cascaded SVRs

for voltage control in a medium voltage power system with a vast number of DGs. The distribution network is partitioned into multiple sections where each equipment is assigned a section to regulate based on the location and operational reach. In addition, cascaded SVRs are also time-graded to ensure those closest to the substation operate first and those furthest from the substation operate last. In [26], a genetic algorithm is proposed to coordinate an OLTC, SVR, capacitor banks and a BESS to regulate voltage and minimize losses. When a voltage rise occurs during off peak period, the OLTC takes priority and keep a certain bus voltage within defined limits. The controller will also issue a charging signal to the BESS. The SVR will be engaged if the OLTC and BESS cannot keep voltage magnitudes within defined limits. To reduce losses and refine power factor, the capacitor bank is switched on if the quantity of reactive power exceeds a specific pre-set limit and switched off if the quantity of reactive power goes below a specific pre-set limit. In [27], a technique is proposed to regulate voltage using a BESS in electric vehicles. The electric vehicles would charge when a high voltage magnitude is detected. When the electric vehicles SOC is not low enough to alleviate the voltage rise, the controller will curtail the active power generated by DGs.

Although the techniques summarised in [14]–[27] are effective in regulating voltage magnitudes to a certain extent, their effectiveness can be enhanced by introducing an average voltage method of voltage regulation instead of a single point voltage regulation method. This is because the methods in literature control the OLTC and SVR with respect to a fixed reference voltage, or a reference voltage computed based on the highest/lowest measured/estimated voltage magnitude. Since the introduction of DGs create a network where the voltage profile of one feeder can have multiple peaks and troughs, regulating voltage based on the peak measured voltage might drop the voltage profile troughs below acceptable limits. Similarly, regulating the voltage based on the measured trough might increase the voltage profile peaks above prescribed limits. In addition, methods proposed in literature uses BESS POC voltage to control the BESS. Therefore, if the voltage peaks/troughs on the voltage profile do not occur where the BESS is connected, the BESS will be underutilized when operating based on its POC voltage.

III. PAPER CONTRIBUTIONS

The proposed method will adopt an average voltage approach. The reference voltage that the OLTC must keep will be calculated from the average voltage of the whole power distribution network that it regulates. Similarly, the reference voltage of the SVR will be computed from the average voltage of the section of the feeder that it regulates. The objective will be to keep the average voltage at nominal voltage. Therefore, based on the computed average voltages, the OLTC and SVR reference voltages will be calculated such that they keep their respective average voltages at nominal voltage. Furthermore, the charging and discharging of the BESS will be controlled based on its POC voltage and the average voltage of the feeder which it is connected to. Therefore, the controller will utilize the BESS when the BESS POC voltage or the feeder average voltage is out of defined limits. The advantage of the average voltage approach is that when DGs are connected, it does not control voltage peaks or voltage troughs of the voltage profile to regulate voltage, it controls their average. By keeping the average voltage at nominal voltage, the controller ensures that voltage peaks do not deviate too far above nominal voltage, and voltage troughs do not deviate too far below nominal voltage. In addition, it is real time, hence, the calculated reference voltages will change to sustain the average voltage at nominal voltage as DG generation and feeder load changes and affect the average voltage. To compute the average voltage, voltage measurements will be taken in locations of the feeder with the potential of experiencing the peak or the lowermost voltage. This include the OLTC bus, DG POCs, BESS POCs, SVR POCs, and the furthest points on feeders. In addition to voltage regulation, the proposed method will also enhance power factor.

Instead of using capacitor banks to boost power factor as implemented in literature, the proposed method will utilize the reactive power of DGs to simultaneously perform voltage control and boost power factor. Lastly, the proposed method will curtail the active power that DGs are producing when voltage magnitudes cannot be kept within acceptable limits. Therefore, the major contributions that this paper present can be summarized as follows.

- Utilize DG reactive power to simultaneously perform voltage control and boost power factor.
- Control the charging and discharging of a BESS based on feeder average voltage and POC voltage.
- Coordinate the OLTC and SVR based on feeder average voltages.
- Curtail DG active power when voltage cannot be kept within acceptable limits.

In operation, the control scheme's sequence will allow DGs to control voltage first, BESS second, SVR third, and OLTC last. The designed control scheme will control the amount of reactive power that the DGs generate based on the DGs POC voltage. Therefore, the POC voltage magnitudes of all DGs will be transmitted to the central controller for the computation of the amount of reactive power each DG must generate through the supervisory control and data acquisition system (SCADA). A BESS charging/discharging algorithm will also be designed that activates the BESS to charge when the POC voltage or the feeder average voltage exceeds a set voltage limit, and activate the BESS to discharge when the POC voltage or feeder average voltage drops below a set voltage limit. In controlling the BESS, the algorithm will ensure that it does not over-charge or completely discharge the BESS as this will damage it. The coordination of the OLTC and SVR will be carried out through a designed sequence that allows the SVR to act first and reach its target voltage or the minimum/maximum tap position before the OLTC can act. The target voltage of both the OLTC and SVR will be

calculated based on real-time voltage magnitudes measured at different locations on the sections of the power distribution network they each control. The coordination of all devices and the computation of all setpoints will be carried out by the central controller using measured parameters transmitted through SCADA.

The layout of the paper will be as follows; Section 1 provided the overview, Section 2 will provide an outline of the impact that OLTCs, SVRs, DGs, and BESS have on power distribution network voltage, Section 3 will provide an overview of the problem statement, Section 4 will assess and discuss the results obtained when the proposed system was evaluated, and Section 5 will provide a conclusion.

IV. OLTC, SVR, DGs, AND BESS IN VOLTAGE REGULATION

A. OLTC AND SVR

The OLTC is the most popular equipment used in South African power distribution networks for voltage regulation. There are both mechanical and electronic OLTCs, however, the electronic OLTCs are expensive and not used often [28]. The South African power distribution network uses only the mechanical OLTCs, hence, this paper and the control scheme proposed will only focus on the mechanical OLTC. The voltage regulation capability of the OLTC arises from its ability to change the power transformer winding ratio [29]. Therefore, as the load through the power transformer changes, and the voltage start changing, the OLTC will change the power transformer winding ratio and prevent the voltage from changing, hence, keeping a constant voltage [30]. The voltage the OLTC controls can be at the power transformer secondary busbar in the substation or at a remote location that is far from the substation where the voltage is estimated through LDC [30].

When operating using its conventional technique, the constant voltage that the OLTC must keep is predetermined and fixed. This fixed reference voltage is determined such that it is high enough to keep the voltage at the point that experiences the lowest voltage during peak load above minimum acceptable voltage. A tolerance margin is also introduced above and below the fixed reference voltage to prevent continuous tap hunting. Therefore, the OLTC must keep its measured voltage within a defined tolerance margin from the fixed reference voltage. However, when distribution feeders being supplied are long, there will be no appropriate fixed reference voltage that can keep the voltage at the furthest points above the minimum prescribed voltage limit, hence SVRs are introduced. The operation of an SVR is similar to that of an OLTC, where they change tap position to keep a local voltage or a remote voltage, estimated through LDC, within defined margins based on a pre-set and fixed reference voltage [31]. However, the OLTC is located at the substation where distribution feeders emanate, and SVRs are installed along a feeder where voltage magnitudes start to drop below the minimum prescribed voltage.

The existing technique that the OLTC and SVR use work effectively in power distribution systems that have no DGs, where the voltage peak is always at the substation, the feeder voltage profile decreases uniformly from the substation, and the maximum voltage drop can be estimated from the peak load and the impedance of the feeder. However, when DGs are introduced, the feeder voltage profile trend becomes nonuniform, and a single feeder can have a voltage profile that has multiple peaks and troughs that will consistently shift based on the generation of DGs. Therefore, under such conditions, a technique that uses a fixed reference voltage, that is determined based on the predictable passive power distribution network will not be effective. An active power distribution network requires an adaptive algorithm that is able to change and adapt as the state of the power network changes. Hence, the algorithm in this paper does not utilize a fixed and static reference voltage, but a variable reference voltage that is calculated based on real time state of the power network.

B. DGs AND BESS

DGs and BESS have certain similarities, both can export active power into the power system. However, unlike common DGs, a BESS can also import active power and charge. In addition, both DGs and BESS can import and export reactive power, however, only DGs will be allowed to export/import reactive power on the scheme designed in this paper. Furthermore, DGs and BESS also affect the voltage, and their impact on voltage can be illustrated by Equations 1-3, where ΔV is the change in voltage between the DG/BESS location and the substation, R is the resistance of a feeder, X is the reactance of a feeder, P_L and Q_L are the active and reactive power drawn by the network load, P_G and Q_G are the active and reactive power exported/imported by DGs/BESS, and V_{OLTC} and V_G are the substation voltage and the voltage where the DG/BESS is connected, respectively [32], [33].

$$\Delta V = \frac{R.P_L + X.Q_L}{V_{OLTC}} + j\frac{X.P_L - R.Q_L}{V_{OLTC}} \tag{1}$$

The imaginary term in Equation 1 is very small in relation to the real term, therefore, Equation 1 can be simplified and represented by Equation 2.

$$\Delta V \approx \frac{R.P_L + X.Q_L}{V_{OLTC}} \tag{2}$$

When DGs are introduced, Equation 2 becomes Equation 3. These are the equations that are used to compute the change in voltage between two points based on the network impedance, load, and DG generated power. Therefore, the voltage rise that will be experienced when DGs are connected is in accordance with Equation 3.

$$\Delta V \approx \frac{R(P_L - P_G) + X(Q_L - Q_G)}{V_G} \tag{3}$$

Equation 2 shows the characteristics of a passive power system with no DGs present. As the line impedance $R + jX$ is known, and the peak load $P_L + jQ_L$ is also known, the voltage

drop between two points ΔV is predictable, and hence voltage regulation is easier. Equation 3 shows the characteristics of an active power system where DGs are present. The change in voltage ΔV will depend on the balance between the active power produced by DGs/BESS, P_G, and the load on the network P_L. Hence, the change in voltage ΔV can be positive, indicating voltage drop, or negative indicating a voltage rise.

Since the power generated by renewable DGs can fluctuate due to their intermittent nature, the change in voltage ΔV is not easy to predict. In addition, when the power generated, P_G is greater than the network load, P_L, the voltage rises, and when P_G is lower than P_L, voltage drops. It is this unpredictability and dynamic nature of a power distribution network with DGs that makes the conventional techniques that rely on predictability inadequate. Furthermore, since the proposed algorithm is tested on a medium voltage grid where $R \approx X$, both reactive power and active power will significantly affect the network voltage as illustrated by Equation 3 [34]. Hence, the balance between the reactive power generated by DGs Q_G and the reactive load Q_L will also affect the voltage. However, the exchange of DG reactive power with the power system to influence voltage will increase the over-all reactive power transmitted by the power system, and hence affect the power system power factor. The power factor is depicted by Equation 4 where PF is power factor, P is active power, S is apparent power and Q is reactive power [32].

$$PF = \frac{P}{S} = \frac{P}{\sqrt{P^2 + Q^2}} \tag{4}$$

A lower power factor indicates a non-efficient power system with high power losses that will lead to excessive voltage drop [35]. Therefore, the scheme designed in this paper will coordinate DGs, BESS, SVR and OLTC to effectively regulate voltage in the presence of DGs and also boost the power factor. The location of a DG on the power distribution network is also significant, as it determines the impact that the DG will have on voltage. DGs that are connected further away from the substation will have the highest impact on voltage. This is because the location furthest from the substation will have the lowest short circuit capacity (SSC), resulting in a weak power network. The SSC is the maximum short circuit current that would flow if a fault occurred at a location. The SSC also determines the strength of a network, where a high SSC indicate a strong network where voltage cannot be easily influenced, whereas a low SSC indicate a weak network where voltage can be easily influenced. The SSC can be expressed by Equation 5 where E is the equivalent voltage and Z is the impedance from the source to the location of assessment [36].

$$SSC = \frac{E}{Z} \tag{5}$$

Since long power distribution lines will have a high impedance towards the end, it will result in a low SSC, and a weak network where DGs can severely impact the voltage. It is this reason DGs connected towards the end of long power distribution lines cause the highest voltage change.

V. PROBLEM STATEMENT

The intermittent nature of renewable power generation creates voltage fluctuation challenges that the OLTC and SVR cannot act fast enough to mitigate. In addition, when the weather conditions are conducive, and the network load is low, the high active power generation by renewable energy sources result in extreme voltage magnitudes that surpass acceptable limits, and the existing technique of the OLTC and SVR is not adequate to suppress them. Since the South African power distribution network has multitudes of long distribution lines, the voltage fluctuations and extreme voltage magnitudes will be worse when DGs are connected. Furthermore, these long distribution lines also experience low voltage magnitudes during peak loading conditions that coincide with low DG generation. These low voltage magnitudes experienced during peak loading conditions are the reason long power distribution lines have SVRs installed. Since these long distribution lines will experience high voltage magnitudes when DGs are generating high active power, and also experience low voltage magnitudes when the peak load is experienced during DG low generation period, a BESS is the optimal equipment to manage voltage regulation.

However, the power distribution network will now have multiple devices regulating voltage including the BESS, OLTC, DGs and the SVR. If not properly coordinated, a conflict will arise between devices, leading to excessive operation and the over-utilization or under-utilization of some devices. Therefore, a system is designed that coordinates DGs, BESS, SVR and OLTC to avert extreme voltage magnitudes and voltage fluctuations. In addition, the designed scheme will regulate the output active power produced by DGs when the BESS, OLTC and SVR fail to maintain acceptable voltage magnitudes. Furthermore, the system will also monitor and boost power factor as the reactive power demand/supply changes with changing voltage magnitudes. Therefore, the objective of the proposed scheme can be defined by Equations 6-9, where f is the objective function, V_n is the nominal voltage, V_{avg} is the feeder average voltage, P_{Gi} and P_{Li} are the generated active power and load, Q_{Gi} and Q_{Li} are the generated reactive power and reactive power demand, V_i and V_k are any two buses that power is transferred between, G_{ik} and B_{ik} are components of the Y bus matrix, V_{min} and V_{max} are the minimum and maximum prescribed voltage limits, respectively, and δ is the voltage angle.

$$f = min\left(\frac{dV_{avg}}{dt}\right) + min\left(\left|V_n - V_{avg}\right|\right) + max\left(\frac{P}{\sqrt{(P^2 + Q^2}}\right) \tag{6}$$

$$\text{s.t } V_{max} \geq V \geq V_{min} \tag{7}$$

$$P_{Gi} - P_{Li} - V_i \sum_{k=1}^{n} V_k \left(G_{ik} cos\delta_{ik} + B_{ik} sin\delta_{ik}\right) = 0 \tag{8}$$

$$Q_{Gi} - Q_{Li} - V_i \sum_{k=1}^{n} V_k \left(G_{ik} sin\delta_{ik} - B_{ik} cos\delta_{ik}\right) = 0 \tag{9}$$

In Equation 6, the first term of minimizing instantaneous voltage change will be achieved by both DGs and BESS since they have a fast response time. Instantaneous voltage change will occur when the weather suddenly changes, when a cloud passes over the photovoltaic plant for solar plants or a sudden drop in wind speed for wind plants. The sudden drop in DG active power generation and the resulting drop in voltage will trigger DGs to export more reactive power and the BESS to discharge and minimize the voltage drop. The second term in Equation 6 of minimizing the difference between nominal voltage and the feeder average voltage is a long-term voltage regulation process that will be achieved by DGs, BESS, SVR and OLTC. As the voltage gradually changes due to a gradually changing load or a gradual change in DG generation, DGs will constantly adjust their reactive power output, BESS will constantly adjust its charging/discharging magnitude, and the OLTC and SVR will constantly change tap position with the objective of keeping the feeders average voltages close to nominal voltage throughout the day.

The last term in Equation 6 of maximizing the power factor will be achieved by DGs as they transfer reactive power to and from the power distribution network. The power factor will be measured at the substation power transformer since that is where the power distribution network total reactive power can be measured. The last term of maximizing power factor is added since DGs that are exporting/importing a small magnitude of reactive power due to low voltage deviation from the nominal voltage at their POC will be made to increase or decrease their reactive power output to compensate for the reactive power demand of those DGs exporting/importing high magnitude of reactive power due to high voltage deviation at their POC, improving the power factor thereof. Equation 7 represent a critical condition that ensures that as the control system operates, all voltage magnitudes are kept between the prescribed maximum and minimum voltage limits. Equations 8-9 are power flow equations that portray the flow of both active and reactive power in a power system [16]. Therefore, to determine the power distribution network bus voltages based on power flow, Equations 8-9 are utilized. Since the proposed control scheme requires several voltage magnitudes, on selected locations to compute its setpoints, those voltages are computed through Equation 8-9. The power distribution network used to assess the proposed control scheme is modelled using Matlab Simulink, hence Matlab Simulink relied on Equations 8-9 to compute selected voltage magnitudes used as inputs to the control system based on active and reactive power flow.

VI. PROPOSED CONTROL SYSTEM

Since the control system is controlling multiple devices, it will use a sequence that prioritizes devices based on response time, robustness, and impact. Since DGs and BESS both have fast response time, DGs are more robust. This is because continuously charging and discharging a BESS can significantly affect its lifespan, whereas continuously exporting and importing reactive power from a renewable DG does not significantly affect its life span. Therefore, DGs will regulate voltage through reactive power first, to minimize the charging-discharging cycles on the BESS, extending the BESS lifespan thereof. The BESS will go second with its charge/discharge capability. The OLTC and SVR also have similar response time and robustness. This is because they are both mechanical, and experience wear and tear when subjected to frequent operation.

However, their impact on the electrical network they regulate is different. The SVR will only change voltage on the section of a feeder that it is connected to, whereas an OLTC has a global impact and changes voltage on all feeders simultaneously. Therefore, the SVR will go third, and the OLTC going last. This is because when voltage on a section of a feeder is well regulated, it improves the overall power distribution system average voltage, and hence reduces the number of tap positions that the OLTC must change. In addition, it has been highlighted in literature that the introduction of DGs will result in excessive tap operation by the OLTC [37]. It is because of this reason that the control system hierarchy allows DGs to regulate voltage first, BESS going second, SVR going third, and OLTC going last. Therefore, by allowing DGs and BESS to regulate voltage first, the number of tap positions that the OLTC and SVR must alter will be reduced when large voltage disturbances occur. When small voltage disturbances occur, DGs and BESS will be able to control them without assistance from the OLTC and SVR.

However, a BESS has a limited lifespan, it is this reason some techniques proposed in the past have limited the BESS to one charge and discharge per day [38]. However, limiting a BESS to one charge and discharge per day will result in the BESS not being available to assist in voltage regulation most of the times, since voltage might rise and drop multiple times a day when DGs are connected, hence reducing the BESS availability factor. Therefore, considering the high price of a BESS, a strategy proposed must ensure that the availability factor of the BESS is high, and the lifespan is long. Therefore, the strategy proposed in this paper suggests the usage of a Vanadium redox battery technology. The Vanadium redox battery technology has a lifespan of up to 10 000 cycles, when cycled to its minimum SOC, this is three times that of lithium-ion that has up to 3000 cycles and ten times that of lead-acid that has up to 1 000 cycles [39]. When not cycled to its minimum SOC, the lifespan of a Vanadium redox battery is longer than 10 000 cycles. A 4MW,6MWh Vanadium redox BESS installed in Tomamae Wind Villa, Japan, has been cycled 270 000 times, down to different SOCs, indicating the robustness of this technology [40]. The overall illustration of the proposed voltage regulation scheme is shown in Figure 1. Based on Figure 1, it can be observed that the central controller receives voltage, active and reactive power measurements from selected locations on the power distribution network. The central controller then computes setpoints for each of its four devices. The operation of each of the four devices that the central controller controls is explained in steps 1-5.

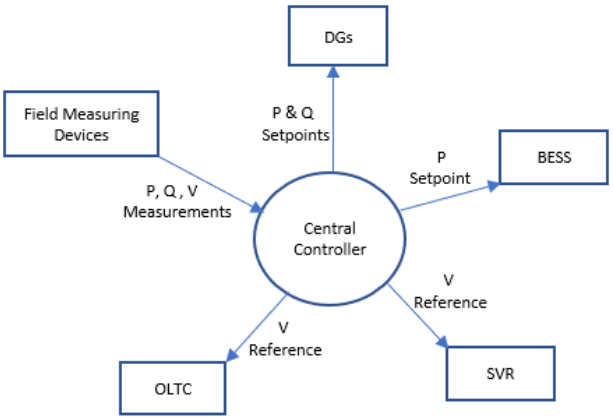

FIGURE 1. Overall illustration of the proposed control scheme.

Step 1: The system will measure voltage where a DG is connected and then determine the quantity of reactive power a DG must absorb/inject to control voltage from Equations 10 where Q_{DG} is the expected reactive power, VDG_{POC} is the DG POC voltage, V_n is the nominal voltage, Q_{max} is the DG maximum reactive power capacity, and S_q is a sensitivity index that illustrates the extent to which voltage is influenced by reactive power where the DG is located.

$$Q_{DG} = \frac{V_n - VDG_{POC}}{S_q} \times Q_{max} \tag{10}$$

A higher S_q resembles a network where voltage is highly influenced by reactive power, and hence a smaller magnitude of reactive power is needed to change voltage. On the other hand, a smaller S_q resembles a network in which voltage is slightly influenced by reactive power, and hence a high reactive power quantity will be needed to change voltage. The sensitivity index S_q is assessed as the ratio between a voltage of 0.01p.u and the amount of reactive power desired to raise the voltage by 0.01p.u at the point of interest. Based on Equation 10, the scheme will instruct a DG to export reactive power when VDG_{POC} is less than V_n and import reactive power when VDG_{POC} is greater than V_n. Therefore, Equation 10 will be utilized by the system to determine the DG reactive power response with respect to voltage for all DGs.

Step 2: The system will control the BESS as shown in Figure 2 where POC_V is the BESS POC voltage and Avg_V is the average voltage of the feeder which the BESS is connected to.

The system will use the voltage magnitude where the BESS is connected and the average voltage of the feeder which the BESS is placed on to determine the magnitude of active power the BESS must discharge/charge. This allows the system to use the BESS not only to regulate BESS POC voltage, but to regulate the entire feeder voltage as well. Therefore, if the BESS POC voltage deviate from defined limits, the system will activate the BESS, similarly, if the feeder average

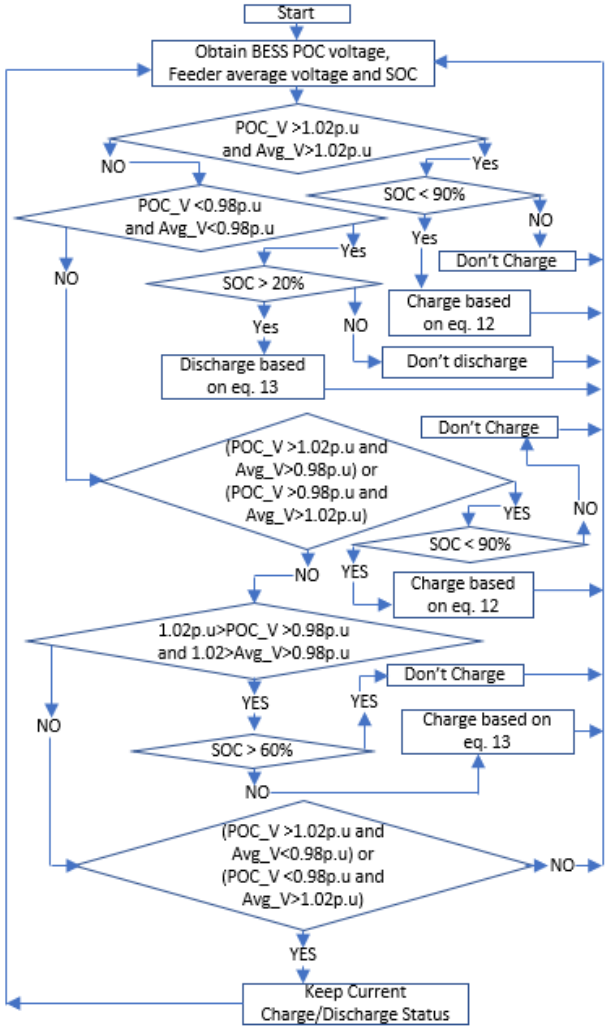

FIGURE 2. Flow chart for BESS control.

voltage deviate from defined limits, the system will activate the BESS.

The feeder average voltage will be computed using all voltage magnitudes measured within the feeder including voltage at the end of a feeder, DGs POC, the secondary and primary side of the SVR, BESS POC and the substation busbar. These are critical locations where the highest or the lowest voltage magnitudes are more likely to occur on a power distribution feeder when DGs are introduced. Hence, using voltage magnitudes from these locations gives an accurate feeder average voltage. Measured voltage magnitudes will be transmitted through the supervisory control and data acquisition system (SCADA). Equation 11 shows how the feeder average voltage is computed where V_{avg} is the feeder average voltage, N is the number of voltage magnitudes measured and V_m is a measured voltage magnitude.

$$V_{avg} = \sum_{1}^{N} \frac{V_m}{N} \tag{11}$$

According to Figure 2, a dead band of 0.02p.u from nominal voltage is given to the operation of the BESS. Therefore, the system will start charging the BESS above 1.02p.u and start discharging the BESS below 0.98p.u. The charging power will increase as the voltage rises further above 1.02p.u, similarly, the discharging power will increase as the voltage moves further below 0.98p.u. However, between 0.98p.u and 1.02p.u, the system can still charge the BESS if the SOC is below 60%. This is to ensure that the BESS does not remain discharged as this will damage the BESS. In addition, between 0.98p.u and 1.02p.u, the system will stop charging the BESS when the SOC reaches 60%. This is to ensure that the BESS is always available to control voltage when either high or low voltage magnitudes occurs, since it will not be in a fully charged or completely discharged state.

Stopping at an SOC of 60% while charging is only applicable when both the POC voltage and the feeder average voltage are between 0.98p.u and 1.02p.u. When either the POC voltage or the feeder average voltage is above 1.02p.u, the system can charge the BESS to an SOC of 90%. As shown in Figure 2, the system will use both the BESS POC voltage and feeder average voltage to control the BESS. If the BESS POC voltage and the feeder average voltage are both above 1.02p.u, and the BESS SOC is above 90%, the BESS will not be charged as this may overcharge and damage the BESS. When the BESS POC voltage and the feeder average voltage are both above 1.02p.u, and the BESS SOC is below 90%, the control scheme will compute the quantity of active power the BESS should import/charge based on the highest voltage magnitude between the BESS POC voltage and the feeder average voltage with a relationship reflected in Equation 12, where P_{BESS} is the desired BESS active power, V_{high} is the defined voltage where the BESS must start charging, V_{POC} is the BESS POC voltage, S_p is a sensitivity index that illustrates the extent to which voltage is influenced by active power at the BESS POC, and P_{rated} is the BESS rated active power. Similar to S_q, the sensitivity of voltage to active power index S_p will be calculated as the ratio between a voltage of 0.01p.u and the amount of active power needed to raise the voltage by 0.01p.u at the POC.

$$P_{BESS} = \frac{V_{high} - max\left(V_{POC}, V_{avg}\right)}{S_p} \times P_{rated} \qquad (12)$$

To ensure that the system does not over charge or completely discharge the BESS, Equation 12 will be implemented in combination with the charging-discharging curve of Figure 3.

The charging-discharging curve of Figure 3 is only applicable above a voltage of 1.02p.u and below a voltage of 0.98p.u. Between 0.98p.u and 1.02p.u, the BESS can only be charged up to an SOC of 60%. As shown in Figure 3, when the SOC exceeds 75%, the charging power will be gradually reduced to prevent overcharging the BESS. The charging will be completely halted when the SOC reaches 90%. The BESS charging is halted at an SOC of 90% since SOC is an estimated variable based on BESS voltage, and

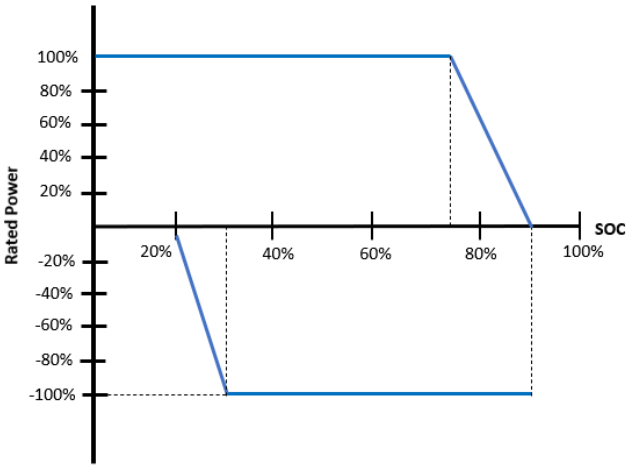

FIGURE 3. BESS charging-discharging curve.

allowing it to get close to 100% increases the chances of overcharging the BESS. The discharging power will also be gradually reduced when the SOC goes below 30% to prevent a complete discharge of the BESS. The discharge will be completely stopped when the SOC reaches 20%. Therefore, after calculating the BESS charging power using Equation 12, the system will utilize the maximum value attained between Equation 12 and Figure 3 based on the BESS SOC.

The maximum value between Equation 12 and Figure 3 is used since the direction of power flow on both Equation 12 and Figure 3 will yield a negative value while charging, and hence the maximum value will be the least magnitude of charging active power. When both the BESS POC voltage and the feeder average voltage are below 0.98p.u, the BESS will need to start discharging to boost voltage magnitudes. The discharging power of the BESS will be in accordance with Equation 13 and Figure 3, where V_{low} is the defined low voltage where the BESS must start discharging. The system will utilize the lowermost discharging power attained between Equation 13 and Figure 3. The minimum value between Equation 13 and Figure 3 is used since the direction of power flow on both Equation 13 and Figure 3 will yield a positive value while discharging, and hence the minimum value will be the least magnitude of discharging active power.

$$P_{BESS} = \frac{V_{low} - min\left(V_{POC}, V_{avg}\right)}{S_p} \times P_{rated} \qquad (13)$$

When either the BESS POC voltage or feeder average voltage is above 1.02p.u, and the other one is above 0.98p.u, the BESS will charge with a charging power determined by Equation 12 and Figure 3. When either the BESS POC voltage or the feeder average voltage is below 0.98p.u, and the other is below 1.02p.u, the BESS will discharge in accordance with Equation 13 and Figure 3. When both the BESS POC voltage and the feeder average voltage are between 0.98p.u and 1.02p.u, the BESS will be charged if the SOC is below 60%. This is to ensure that the BESS does not remain in a

discharged state, but it is still able to charge should a high voltage magnitude be detected. The charging power between 0.98p.u and 1.02p.u will be in accordance with Equation 13. Although Equation 13 was used to calculate the discharging power when the measured voltage is below V_{low}, it can also be used to calculate the charging power when the measured voltage magnitude is above V_{low}, but below V_{high}. This is between 0.98p.u and 1.02p.u. Therefore, Equation 13 will also be used to calculate the charging power when both the BESS POC voltage and the feeder average voltage magnitudes are between 0.98p.u and 1.02p.u.

Equation 13 ensures that the charging power between a voltage of 0.98p.u and 1.02p.u does not cause the lowest voltage magnitude between the BESS POC and the feeder average voltage to drop below 0.98p.u. In addition, when charging the BESS when both the BESS POC voltage and the feeder average voltage are between 0.98p.u and 1.02p.u, the charging-discharging curve of Figure 3 is not applicable, since charging will stop when SOC gets to 60%. When either the BESS POC voltage or feeder average voltage is above 1.02p.u and the other is below 0.98p.u, the system cannot use the BESS to control voltage, hence the BESS will keep its current state. This is because regulating one voltage will worsen the other. To incorporate Equation 12 for charging when the voltage is above 1.02p.u, Equation 13 for discharging when voltage is beneath 0.98p.u, Equation 13 for charging when voltage is between 0.98p.u and 1.02p.u, and Figure 3, a fuzzy logic controller was used. When determining the active power rating of the BESS to be installed, the efficiency of the battery technology in use must be considered. Therefore, the active power rating of the BESS to be installed must be calculated based on Equation 14, where $BESS_P$ is the BESS active power rating, P_{Calc} is the active power required to boost/suppress voltage calculated based on network voltage sensitivity, and η is the battery technology efficiency in per unit.

$$BESS_P = P_{Calc} + (P_{Calc} \times (1 - \eta)) \tag{14}$$

Using Equation 14 will ensure that the BESS installed can deliver the active power required. If the efficiency of the BESS is not considered, the BESS installed will deliver a small amount of active power than required.

Step 3: The system will control the SVR and the OLTC from attained average voltage magnitudes. The SVR will use the average voltage obtained from measuring voltage magnitudes on the section of the feeder that it regulates. These voltage magnitudes will include voltage at the end of the feeder, DGs and BESS POCs, and the location where the SVR is connected on both its secondary and primary sides. The system will also control the OLTC based on the average voltage of all feeders connected to it. The locations where voltage will be measured will include the DG POC, BESS POC, SVR POC, substation busbar and the end of feeders. These points will be measured in all feeders that the OLTC is regulating. The reason for measuring voltage in these locations is that they are the critical locations where the highest or the lowest voltage magnitudes are more likely to occur when DGs are introduced. Therefore, computing an average voltage based on the highest and lowest voltage magnitudes gives a more accurate average voltage. Based on all voltage magnitudes that have been measured in different locations, the control scheme will then determine the average voltages and the reference voltages for both the SVR and OLTC in accordance with Equations 15 and 16 where V_{SVR} and V_{OLTC} are the SVR and OLTC reference voltages, respectively, V_p is any voltage magnitude measured within the section the SVR is regulating, V_a is any voltage magnitude measured within all feeders the OLTC is regulating, N is the number of voltage magnitudes measured within the section of the feeder the SVR is regulating, M is the number of voltage magnitudes measured in all feeders the OLTC is regulating, and V_n is the nominal voltage.

Equation 15 will compute the SVR reference voltage such that the average voltage of the section the SVR regulates is close to nominal voltage. Similarly, Equation 16 will compute the OLTC reference voltage such that the average voltage of the feeders the OLTC regulates is close to nominal voltage. Since Equations 15 and 16 uses real time voltage magnitudes to produce the reference voltages, the reference voltages will not stay fixed, they will change with respect to the measured voltage magnitudes. Therefore, the control system will ensure that the SVR and the OLTC changes their tap positions to match their respective reference voltage with the measured voltage where they are located. To prevent tap position hunting, an error margin will be introduced. Therefore, for the tap position change signal to stop, the measured voltage must be within a defined tolerance margin from the calculated reference voltage.

$$V_{SVR} = \sum_{a=1}^{N} \frac{V_n - V_p}{N} + V_n \tag{15}$$

$$V_{OLTC} = \sum_{a=1}^{M} \frac{V_n - V_a}{M} + V_n \tag{16}$$

To avoid concurrent operation between the SVR and the OLTC, which might lead to conflict between equipment, the OLTC will wait for the SVR to match its computed reference voltage with its POC voltage or reach the minimum/maximum tap position. Once the SVR has matched its computed reference voltage with its POC measured voltage or has reached maximum/minimum tap position, the system will activate the OLTC. The flow chart of Figure 4 shows the SVR and OLTC sequential operation where *Ref_V* is the SVR computed reference voltage and *V_SVR* is the voltage measured on the secondary side of the SVR.

As shown in Figure 4, the OLTC will wait for the SVR to equalize its reference voltage with the measured voltage or reach the maximum/minimum tap position before it starts. The sequence of allowing the SVR to control voltage first will allow feeder voltage magnitude to improve before the OLTC start regulating, as the OLTC regulate multiple feeders simultaneously and the SVR regulate one feeder. Therefore, if high voltage magnitudes are experienced in a feeder, the SVR will suppress the high voltage magnitude first. This will reduce

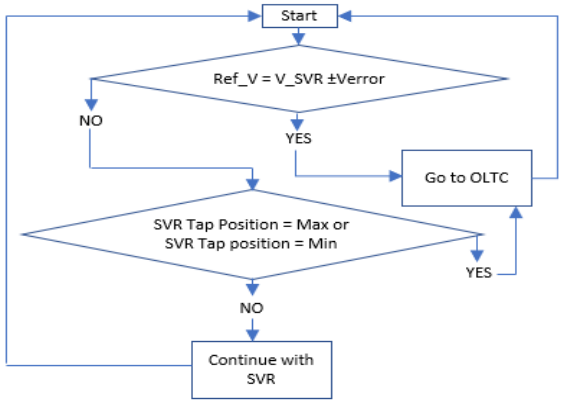

FIGURE 4. SVR and OLTC operational sequence.

the number of tap positions the OLTC has to change. In operation, both the SVR and OLTC will change tap positions until the reference voltages calculated in Equations 15-16 are within a defined error margin from their respective measured POC voltages or they have reached minimum/maximum tap position.

Step 4: If the procedures defined in steps 1-3 cannot successfully reduce a DG POC voltage below the upmost prescribed voltage V_{max}, the system will reduce the active power generation of the DG located at that point where the voltage is still above V_{max}. The system will calculate the DG active power based on Equation 17, where P_{export} is the new active power value the DG must generate and export after the active power reduction process, P_{Gen} is the initial active power value that the DG is generating and injecting to the distribution network before the active power reduction process, V_{max} is the upmost prescribed voltage limit, V_{error} is the prescribed error margin above V_{max}, VDG_{POC} is the DG POC voltage, and S_p is the sensitivity index that illustrates the impact active power has on the voltage at the DG POC.

$$P_{export} = P_{Gen} - \left(\frac{VDG_{POC} - (V_{max} + V_{error})}{S_p} \times P_{Gen} \right) \tag{17}$$

Based on Equation 17, the amount of DG output active power reduced will be proportional to the difference between the DG voltage at its POC and the upmost prescribed voltage V_{max}. A high difference between the two voltage magnitudes will prompt a higher reduction in active power produced by the DG. The control system will follow the sequence of Figure 5 in reducing the active power of DGs where *Ref_V_SVR* is the SVR reference voltage, *V_SVR* is the SVR measured voltage, *Ref_V_OLTC* is the OLTC reference voltage, *V_OLTC* is the OLTC measured voltage and $P_{available}$ is the peak possible power a DG can generated based on primary energy source availability. An error margin V_{error} will also be introduced above V_{max} to prevent DGs from reducing active power generation when the voltage

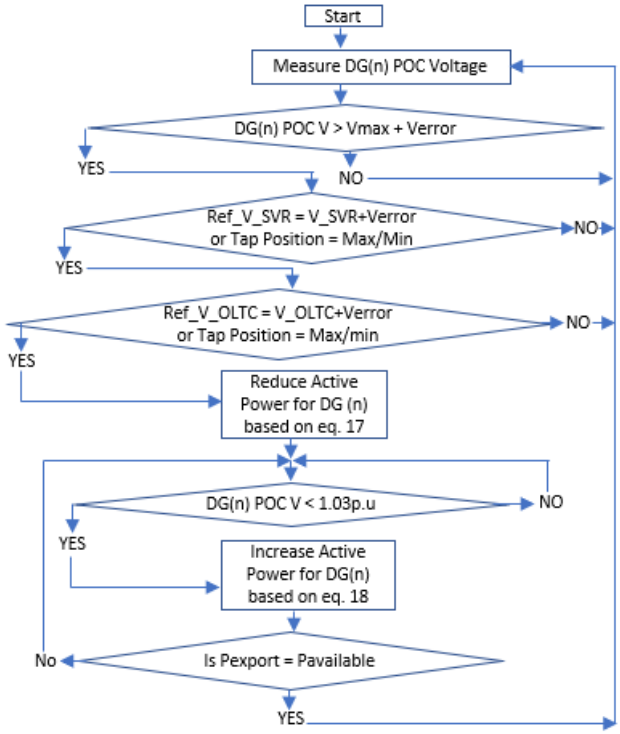

FIGURE 5. DG active power reduction/recovery process.

could still recover. However, when the voltage goes beyond $V_{max} + V_{error}$, and the OLTC and SVR have operated, the chances of voltage recovery are slim. Therefore, DGs will only be instructed to reduce active power generation when their POC voltage has surpassed $V_{max} + V_{error}$, and the OLTC and SVR cannot act.

The operation of the process in Figure 5 can be explained as follows. If a voltage above $V_{max} + V_{error}$ is measured at any DG POC, the system will assess the state of the OLTC and SVR before proceeding to reduce active power production for that DG.

It is only when the voltage at the DG POC is still higher than $V_{max} + V_{error}$, and both the SVR and OLTC have equalized their calculated reference voltages with the measured voltages or have reached minimum/maximum tap position that the system will issue an instruction for the DG linked to that respective POC to reduce active power generation and also calculate the new active power value that the DG must reduce to. Checking for the SVR and OLTC status is done to ensure that all voltage regulation measures have taken place, and high voltage is persistent. If these checks are not performed, the system might reduce the DG active power unnecessarily when the voltage regulation equipment could have successfully regulated voltage to acceptable range. Reducing DG active power generation reduces revenue, demotivate investors from building more DGs, and decelerate the world's objective of moving towards renewable energy. Therefore, reducing DG active power generation will only be done when there is no other option to curb rising voltage magnitudes.

In reducing active power generation, the system will use Equation 17.

To ensure that the DG does not get caught in a loop of continuously increasing and decreasing active power generation, the system will only attempt to increase active power once the DG POC voltage goes below 1.03p.u. The increase of DG active power once the DG POC voltage has gone below 1.03p.u will be in accordance with Equation 18, where P_{export} is the new active power value that the DG must generate and export after the active power increment process, and P_{Gen} is the active power value that the DG is producing right before the active power increment process is carried out.

$$P_{export} = P_{Gen} + \left(\frac{V_{max} - VDG_{POC}}{S_p} \times P_{Gen} \right) \quad (18)$$

Since Equation 18 will only attempt to increase active power of a DG such that the DG POC voltage does not exceed V_{max}, it might not increase active power to the level it was before reduction. However, modern renewable DGs can compute their peak possible/available power based on primary energy source availability, e.g. wind speed or solar irradiance. Therefore, the system will continuously compare the active power the DG is generating with the DG peak possible/available active power based on weather conditions. If the active power the DG generates after increasing power generation has not reached possible/available peak power due to voltage constraints, the system will monitor the DG POC voltage and keep trying to increase active power generation as the voltage drops until generated power is similar to the calculated peak possible/available power. However, the system will not force the DG to violate voltage limits in effort to increase active power generation.

Step 5: Since modern DGs have reactive power capability and can influence voltage through reactive power as demonstrated in step 1, the exportation and importation of reactive power in effort to support voltage alters the power system power factor. The proposed control scheme has a strategy to improve this power factor that will be reduced as DGs import/export reactive power to control voltage. Therefore, DGs that are not participating in voltage control through reactive power or those that are exporting/importing a trivial magnitude of reactive power due to low voltage deviation from nominal voltage at their POC will be used to compensate the power distribution network reactive power demand, and boost the power factor. DGs exporting/importing high magnitude of reactive power due to high voltage deviation from nominal voltage at their POC cannot be used for power factor correction, as this might make their voltage deviation worse. Furthermore, DGs exporting/importing high reactive power magnitude to control voltage are the ones with a negative impact on the power system power factor. It is this reason that only DGs with a POC voltage deviation that requires a reactive power output less than 30% of the DG reactive power rating will be nominated for power factor correction. These DGs are nominated since importing/exporting a low magnitude of reactive power indicate that they do not have voltage problems where they are connected. Therefore, the control system will give these DGs new reactive power setpoints that allows them not to control voltage only, but also enhance the power system power factor. These DGs that are exporting/importing low reactive power to regulate voltage are then used as capacitors/inductors to provide/consume extra reactive power to enhance power system power factor.

While performing power factor correction, the control scheme will depend on the reactive and active power that passes through the substation power transformer to compute the power factor. Once the power system power factor has been computed, the system will select DGs it will utilize to boost the power factor. As stated earlier, the scheme will select those DGs with a POC voltage deviation that requires a DG reactive power output less than 30% of the DG reactive power rating. DGs with a POC voltage deviation that requires reactive power output equal or greater than 30% of the DG reactive power rating will be solely focused on controlling voltage. The control scheme will then compute power factor enhancement setpoints for selected DGs based on Equations 19-22. Equation 19 will be used to assign the maximum reactive power that each nominated DG must export/import, where Q_{DG} is the maximum power factor enhancement reactive power that each nominated DG must generate to completely correct the power factor at the substation, $Q_{Measured}$ is the total distribution system reactive power demand measured at the substation, and z is the total number of DGs nominated for power factor enhancement [15]. Therefore, Equation 19 will determine the maximum reactive power that each DG selected for power factor refinement must export/import to enhance power factor back to unity. Equation 19 will also ensure that the reactive power to be compensated is evenly distributed through all DGs selected for power factor enhancement.

$$Q_{DG} = \frac{Q_{Measured}}{z} \quad (19)$$

However, the system will need to confirm if each of the nominated DGs can export/import the required maximum reactive power Q_{DG} considering the POC voltage. The system will then use Equations 20-21, where $Q_{possible}$ is the possible peak reactive power a DG is able to exchange with the network considering its POC voltage, VDG_{POC} is the DG POC voltage, V_{max} and V_{min} are the upmost and lowermost prescribed voltages, respectively, Q_{max} is the DG maximum rated reactive power capacity, and S_q is the sensitivity index illustrating the influence reactive power has on POC voltage.

$$Q_{Possible} = \left(\frac{V_{min} - VDG_{POC}}{S_q} \right) \times Q_{max}, \quad Q_{Measured} < 0 \quad (20)$$

$$Q_{Possible} = \left(\frac{V_{max} - VDG_{POC}}{S_q} \right) \times Q_{max}, \quad Q_{Measured} > 0 \quad (21)$$

Once the system has determined the reactive power each DG is capable of generating without exceeding the prescribed voltage magnitudes V_{max} and V_{min}, it will then compare Equations 19 and 20, and utilize the highest value, or compare Equations 19 and 21, and use the lowest value. The decision to either compare Equation 19 with Equations 20 or 21 will depend on the direction of reactive power measured at the substation transformer. Therefore, DGs nominated for power factor correction will be exporting/importing a sum of two reactive power magnitudes, which is the reactive power for voltage regulation given by Equation 10, and the reactive power for power factor enhancement given by Equations 19-21. Therefore, the reactive power setpoint for a DG nominated for power factor enhancement can be represented by Equation 22, where Q_{V_PF} is the nominated DG reactive power setpoint, Q_V is the reactive power for controlling voltage computed based on Equation 10, and Q_{PF} is the reactive power for power factor enhancement computed based on Equations 19-21.

$$Q_{V\_PF} = Q_V + Q_{PF} \tag{22}$$

However, as a DG selection criterion for it to be eligible for boosting power factor, the reactive power for controlling voltage, Q_V, will be small, and below 30% of the DG reactive power rating. The reactive power setpoints of DGs not selected for power factor enhancement will be computed based on Equation 10 only.

Since exporting/importing below 30% of the DG maximum rated reactive power is a requirement for it to be eligible for power factor enhancement, POC voltage getting close to V_{max} or V_{min} will be the criteria for withdrawing a DG from power factor enhancement. To ensure that the minimum and maximum prescribed voltage limits are not violated, the controller will withdraw a DG from power factor correction when its POC voltage gets to $(V_{max} - 0.01p.u)$ or $(V_{min} + 0.01p.u)$. Once a DG is withdrawn from power factor correction, the controller will use it solely for voltage regulation in accordance with Equation 10, until it meets the requirements of being used for both voltage regulation and power factor refinement again, in accordance with Equation 22. Furthermore, when the power factor as measured at the substation power transformer is above 0.98, the controller will not engage any DG for power factor enhancement.

VII. RESULTS AND ANALYSIS

To assess the efficiency of the proposed scheme, two South African 22kV lines that are supplied from the same substation were used as shown in Figure 6. The substation consists of a 132/22kV, 40MVA, power transformer fitted with an OLTC. One feeder has an SVR installed. DGs were also added to the feeders. These DGs were added based on the network SSC, since the network voltage is easily influenced by active and reactive power where the SSC is low, and resistant to change where the SSC is high [5]–[7]. Hence, DGs were distributed through areas of medium and low SSC. Since the highest SSC

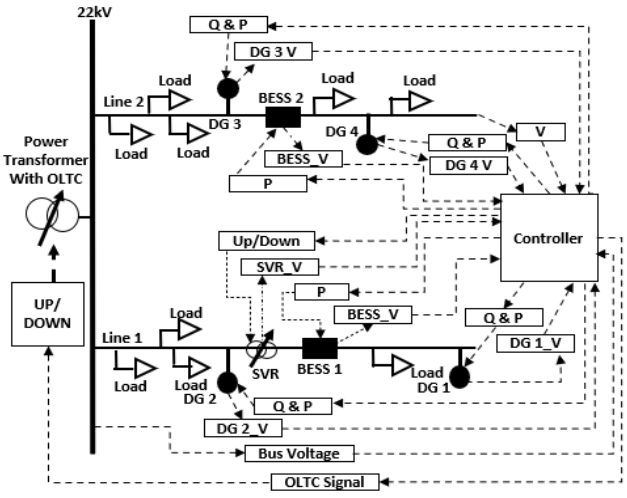

FIGURE 6. A power distribution network with DGs, BESS, SVR, OLTC and controller interconnections.

of a power distribution network is at the substation busbar, and it reduces with the length of the feeder. The area of medium SSC was identified at the middle of the feeder, and the area of low SSC towards the end of the feeder. Therefore, DGs were located in the middle, and towards the end of the feeder. The reason for distributing DGs in areas of medium and low SSC was to observe the highest change in voltage magnitudes. In addition, in real world operation, it is the DGs in medium and low SSC networks that cause the highest change in voltage magnitudes, and this control system was intended to alleviate that problem.

The maximum rated reactive power capacity of all DGs will be in relation to the South African grid connection code for renewable power plants which dictates that category B plants should have reactive power capacity that is 22.8% of their maximum rated active power [41]. A BESS was also added to both feeders. To ensure that the BESS assist the network during high DG generation period that coincide with low loading conditions, and during low DG generation period that coincide with peak loading conditions, the BESS was located at a point on the feeder where the voltage breaches the minimum prescribed voltage V_{min}, during feeder peak load, and in the absence of DG generation. Therefore, the location of the BESS will be remarkably close to the location of the SVR. The rating of each of the two BESS was decided based on the sensitivity index S_p that illustrates the impact of active power on voltage where the BESS is located.

Since the BESS is placed in a location of the feeder where voltage breaches V_{min}, the BESS must have enough active power such that it can boost the voltage from V_{min}, to a value above nominal voltage. The minimum prescribed voltage, V_{min}, will be taken as 0.95p.u, and the value above nominal voltage will be taken as 1.03p.u. Through simulation, it was discovered that 0.45MW of active power is required to raise the voltage by 0.01p.u where BESS 1 is placed on

feeder 1. Hence, BESS 1 must have a minimum output power of 3.6MW in order to change the voltage from 0.95p.u to 1.03p.u where it is connected. Similarly, 0.51MW of active power is required to raise the voltage by 0.01p.u where BESS 2 is connected on feeder 2. Hence, BESS 2 must have a minimum output power of 4.08MW in order to raise the voltage from 0.95p.u to 1.03p.u. Considering a 90% efficiency for the battery technology in BESS 1, and 80% efficiency for the battery technology in BESS 2, BESS 1 was designed to be a 4MW/12MWh system, and BESS 2 was designed to be a 5MW/15MWh system. The maximum DG active power output was set to 7MW, this was the power required to cause reverse power flow and excessive voltage magnitudes given the loading on feeders 1 and 2. Figure 6 shows the power distribution network utilized.

Two 22kV feeders are supplied by the power transformer as shown in Figure 6, and feeders 1 and 2 are 69km and 57km long, respectively. The load on feeders 1 and 2 is 8.43MW and 6.78MW, respectively. The interconnections between the proposed controller and the power distribution network equipment are also illustrated. The power distribution network of Figure 6 is simplified to show the interconnections, the real feeders extend outwards in a complex tree-like structure. Furthermore, in simulation, the real-world operation time of equipment was accelerated for better analysis and presentation of results. However, this does not affect their impact on the power system. Hence, the response of the power system will still mimic that of a real-world power system.

To minimize the amount of data transmitted through SCADA, and avoid computational complexity, the proposed control scheme will use a 1 second average value to perform computations. Therefore, for all measured variables in different locations, including voltage magnitudes, active power, and reactive power, only one value per measured variable will be transmitted to the central controller every second. This one value per measured variable sent per second, will be the average of multiple points sampled within the continuous signal of the measured variable on that second. This means that, for all measured locations that have been selected, each one of them will transmit its 1 second average measured value to the central controller every second. The period which one value per measured variable is sent to the central controller will be adjustable to cater for communication networks with a slow data transmission rate. The assessment of the system will be carried out through a series of four scenarios. These four scenarios will demonstrate different attributes of the proposed system.

A. SCENARIO 1: A NETWORK WITH DGs AND USING CONVENTIONAL VOLTAGE REGULATION METHOD

Scenario 1 will evaluate a network in which the OLTC and SVR are operating based on their conventional technique, where they regulate voltage based on a pre-set and fixed reference voltage. The fixed reference voltage for both the OLTC and SVR will be 1.03p.u. This is a reference voltage commonly used on South African medium voltage power

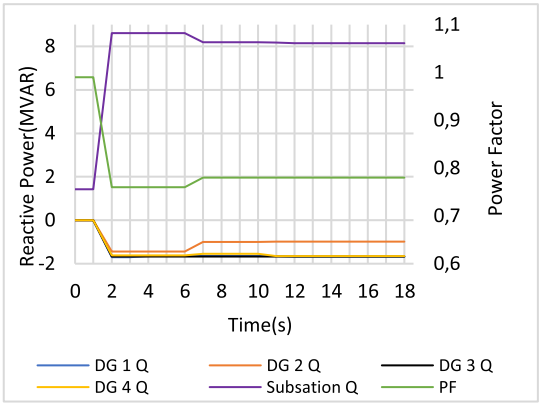

FIGURE 7. DGs reactive power and substation power factor for scenario 1.

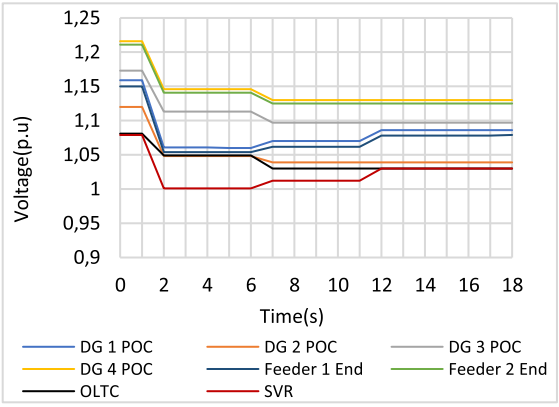

FIGURE 8. Power distribution system voltage magnitudes for scenario 1.

distribution network tap changing transformers. In addition, DGs will export active power and also regulate voltage through reactive power in accordance with their POC voltage. The network of assessment will be similar to that portrayed in Figure 6, with the BESS, controller and the controller interconnections removed. This scenario will evaluate the response of the conventional technique when DGs are generating constant active power with DGs 1-4 generating 6.32, 6.75, 5.96, and 6.1MW, respectively. The DGs reactive power output and the resulting distribution network voltage magnitudes are shown in Figures 7-8.

Initially, at t = 0 s, DGs are exporting active power to the power system with a reactive power output of 0 Mvar as illustrated in Figures 7. The constant active power exported by DGs increased voltage magnitudes on several locations of the power distribution system with the highest measured voltage being 1.216p.u at the DG 4 POC, and the lowest measured voltage being 1.079p.u at the SVR location as shown in Figure 8. All voltage magnitudes measured and displayed at t = 0 s in Figure 8 are classified as high voltage magnitudes, as most power utility companies around the world try to keep medium voltage networks voltage deviation below 5% of nominal voltage. Using their reactive power capability, DGs imported reactive power in an attempt to repress voltage

magnitudes at t = 2 s, as shown in Figure 7. DGs 1-4 imported 1.64, 1.44, 1.67, and 1.62Mvar, respectively. However, only DG 2 managed to bring its POC voltage within 5% of nominal voltage at 1.048p.u. The rest of the DG POC voltage magnitudes and the voltages at the end of feeders were still above 1.05p.u. The DGs importation of reactive power presented in Figure 7, at t = 2 s, also dropped the power factor from 0.99 to 0.76.

The voltage magnitudes that were measured at the SVR and OLTC locations had also dropped below 1.05p.u, to 1.001 and 1.049p.u, respectively. Since the OLTC and the SVR local voltage magnitudes were at 1.049p.u and 1.001p.u, and their fixed reference voltage is 1.03p.u, they started changing tap positions. They also changed tap positions simultaneously, at t = 6 s since there is no coordination. Since the OLTC measured voltage is at 1.049p.u, it moved its tap position once, and took the voltage down to 1.032p.u. The OLTC measured voltage is now at 1.032p.u, which is within a 0.01p.u tolerance margin from the fixed reference voltage of 1.03p.u, therefore, no further tap position change would be required from the OLTC. On the other hand, the SVR measured voltage was at 1.001p.u, hence, it also moved its tap position once and take the voltage up to 1.012p.u in effort to get to its reference voltage. Since the SVR measured voltage was at 1.012p.u, and not within a declared tolerance margin from its reference voltage of 1.03p.u, a second tap position change was initiated at t = 11 s. The SVR then stepped the voltage up one more time from 1.012p.u to 1.03p.u, and then stopped since the measured voltage was now within a margin of 0.01p.u from the fixed reference voltage as shown in Figure 8.

However, while stepping up the voltage from 1.001p.u to 1.03p.u in effort to reach its fixed reference voltage, the SVR also stepped up the voltage at the DG 1 POC from 1.061p.u to 1.086p.u. Furthermore, the voltage at the end of feeder 1 was also elevated from 1.054p.u to 1.078p.u during the same SVR operation. Therefore, the SVR has made the voltages at the DG 1 POC and the end of feeder 1 worse than they were before the SVR operation. It is this reason that makes the OLTC and SVR that uses a fixed reference voltage ineffective when DGs are connected. In addition, the OLTC stopped at its fixed reference voltage of 1.03p.u while voltage magnitudes throughout the power distribution network were still high, with the highest measured voltage of 1.13p.u at the DG 4 POC, and the lowest of 1.030p.u at the SVR POC. Given that the OLTC had not reached minimum/maximum tap position, and the lowest measured voltage is 1.030p.u, which is still far from the prescribed minimum voltage of 0.95p.u, the OLTC should be able to reduce voltage magnitudes further and regulate 1.13p.u further down. However, its static voltage regulation philosophy does not allow it to do so. It is because of these reasons that the control system presented in this paper does not utilize a fixed reference voltage but calculate appropriate reference voltages that the OLTC and SVR must follow based on real time voltage magnitudes. Furthermore, the power factor only improved to 0.78 when the conventional method has acted as shown in Figure 7. Renewable DGs are also intermittent, therefore, instead of generating constant active power, they can also generate fluctuating active power. Hence, a sudden reduction in DG active power generation may cause sudden reduction in voltage magnitudes within the network which the mechanical SVR and OLTC used in South African networks cannot act fast enough to alleviate. Therefore, the proposed scheme will utilize a BESS to lessen the impact of DGs fluctuating active power on the power distribution system.

B. SCENARIO 2: A NETWORK WITH DGs, BESS, SVR AND OLTC USING THE PROPOSED CONTROL SYSTEM

This scenario will utilize the set-up portrayed in Figure 6 with DGs, BESS, SVR and the OLTC controlling the network voltage, and boosting the network power factor based on the proposed control algorithm. The active power generated by DGs will be similar to that in scenario 1, with DGs 1-4 exporting 6.32, 6.75, 5.96, and 6.1MW, respectively. The same high voltage magnitudes experienced at the beginning of scenario 1 will also be experienced at the beginning of scenario 2. This will provide a good comparison of the conventional technique and the proposed system. The BESS SOC was set to 50% for both BESS 1 and 2. The results are shown in Figures 9-14.

At the beginning, t = 0 s, there are high voltage magnitudes measured on several sites of the power distribution network with the highest measured voltage being 1.216p.u at the DG 4 POC, and the lowest being 1.079p.u at the SVR location. This is clearly depicted at the beginning of Figures 9, 10, 12, 13, and 14. These voltages are categorized as high voltage magnitudes since most power utility companies wish to keep medium voltage networks voltage deviation below 5% of the nominal voltage. Based on its sequence, the controller allowed DGs to absorb reactive power from the network and control voltage first, hence, DGs 1-4 imported 1.64, 1.44, 1.67 and 1.62Mvar, respectively as shown in Figure 11, at t = 2 s. Their effort managed to suppress voltage magnitudes slightly, as the highest measured voltage magnitude reduced to 1.146p.u at the DG 4 POC, and the lowest recorded voltage magnitude reduced to 1.001p.u at the SVR location as shown in Figures 10 and 14. At this point, the power factor reduced from 0.99 to 0.82 as shown in Figure 11.

The second phase for the controller is to activate the BESS. At this point, BESS 1 and 2 POC voltages were at 1.009 and 1.118p.u, respectively. In addition, the average voltage magnitudes for feeders 1 and 2 were 1.043 and 1.130p.u, respectively. Since the scheme uses both the BESS POC voltage and the average voltage of the feeder which the BESS is connected to, it calculated that BESS 1 and 2 must charge with 2.86 and 4.63MW, respectively, to suppress voltage magnitudes at t = 4 s as shown in Figures 12-13. In this instance, the controller used the feeder average voltage to calculate the charging power since the average voltage was higher than the POC voltage. However, the controller ensured that the BESS

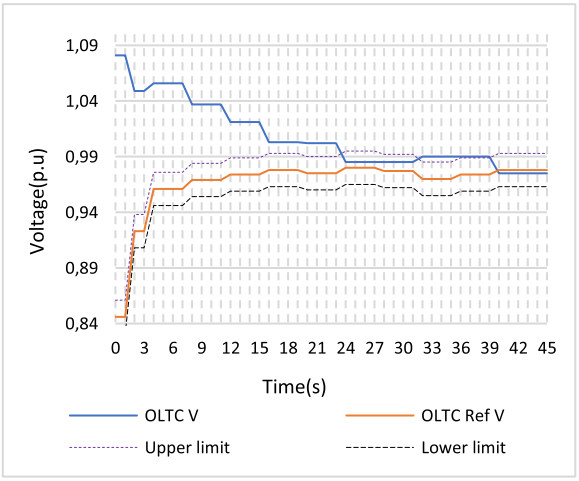

FIGURE 9. OLTC measured and calculated reference voltage for scenario 2.

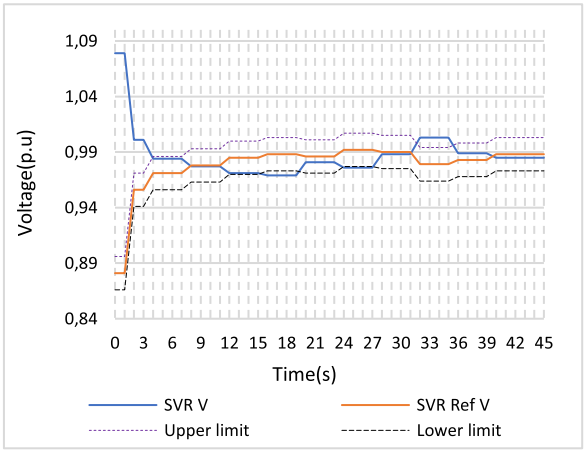

FIGURE 10. SVR measured and calculated reference voltage for scenario 2.

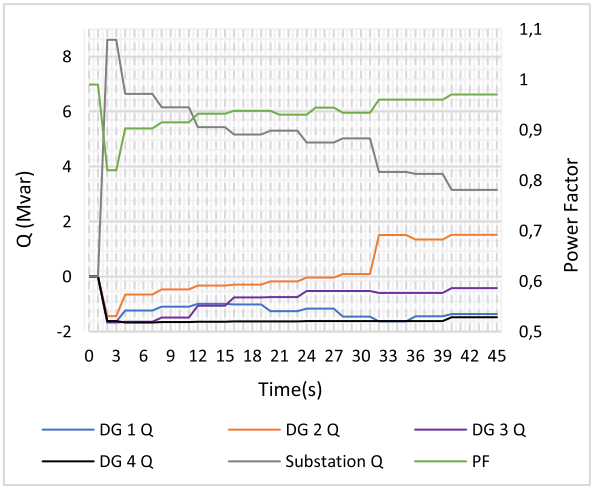

FIGURE 11. DG reactive power, substation reactive power and power factor for scenario 2.

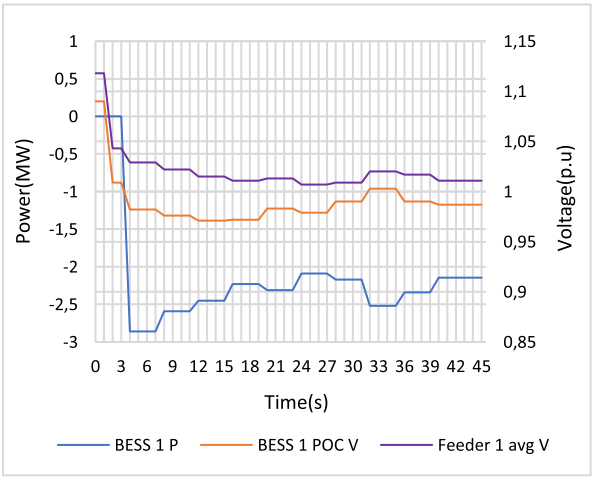

FIGURE 12. BESS 1 output power, POC voltage and feeder 1 average voltage for scenario 2.

POC voltage does not drop below V_{low}. In addition, BESS 2 charged with a higher active power magnitude than BESS 1 since the feeder average voltage where it is connected was higher than that of BESS 1. The action by BESS 1 and 2 reduced the power distribution network voltages further, and the highest measured voltage was now 1.083p.u at the DG4 POC, and the lowest measured voltage 0.984p.u at the SVR location.

The next phase of the controller after controlling DGs and BESS, is to control the mechanical devices including the SVR and the OLTC. The SVR is controlled first, and the OLTC will only be controlled once the SVR has reached its calculated reference voltage or has reached minimum/maximum tap position. A tolerance margin of 0.015p.u will be allowed for both the OLTC and SVR, therefore, the controller will stop changing tap position once the measured voltage is within 0.015p.u from the calculated reference voltage for both the OLTC and SVR. As shown in Figure 10, at t = 4 s, the SVR was at a measured voltage of 0.984p.u which is within 0.015p.u from its calculated reference voltage of 0.971p.u. This indicates that the action of DGs and BESS has matched the SVR measured and calculated reference voltages. Therefore, the controller moves to the OLTC. It calculated the OLTC reference voltage of 0.961p.u using the received measured voltage magnitudes and Equation 16. Since the OLTC measured voltage was at 1.056p.u, a tap position change was initiated. The OLTC then altered its tap position from tap 4 to 5, and its measured voltage reduced to 1.037p.u at t = 8 s as shown in Figure 9.

The controller recomputed the OLTC reference voltage to 0.969p.u, and since the measured voltage was 1.037p.u, another tap position change was required. Before the controller can enable the OLTC for a second tap position change, it checked if the SVR is still within its calculated reference voltage. Since the SVR was at a measured voltage of 0.977p.u, and its calculated reference voltage at 0.978p.u, they were within 0.015p.u from each other as shown at t = 8 s in Figure 10. Therefore, the OLTC moved from tap 5 to

tap 6, moving the voltage from 1.037p.u to 1.021p.u. A new OLTC reference voltage was calculated to 0.974p.u. Since the SVR was still within the defined tolerance from its calculated reference voltage, a third OLTC tap position change to tap 7 was carried out. This moved the OLTC measured voltage further from 1.021p.u to 1.003p.u as shown at t = 16 s in Figure 9. At this point, the SVR measured voltage drifted to 0.969p.u which was no longer within 0.015p.u from the SVR calculated reference voltage of 0.988p.u, as shown at t = 16 s in Figure 10. Therefore, the controller paused the OLTC and changed the tap position of the SVR once, this changed the SVR voltage from 0.969p.u to 0.981p.u, as shown at t = 20 s in Figure 10. Since the SVR measured voltage was now at 0.981p.u, and its calculated reference voltage at 0.986p.u, they were within 0.015p.u from each other. Therefore, the controller went back to adjusting the OLTC. The OLTC measured voltage was at 1.002p.u, and the calculated reference voltage at 0.975p.u. The controller then moved the OLTC to tap 8, moving the measured voltage from 1.002p.u to 0.985p.u. At this point, the OLTC measured voltage was within 0.015p.u from its calculated reference voltage of 0.980p.u, as shown at t = 24 s in Figure 9. However, the SVR at 0.976p.u has drifted away by more than 0.015p.u from its calculated reference voltage of 0.992p.u, as shown at t = 24 s in Figure 10. The controller then changed the SVR tap position a second time taking the SVR measured voltage from 0.976p.u to 0.988p.u, which is within 0.015p.u from the calculated reference voltage of 0.990p.u.

At this point, both the OLTC and SVR measured voltages were within 0.015p.u from their calculated reference voltage as shown at t = 30 s in Figures 9-10. After the operation of the DGs, BESS, SVR and the OLTC using the proposed control system, the highest voltage magnitude measured was 1.051p.u at the DG 4 POC, and the lowest measured voltage was 0.988p.u at the SVR location. In scenario 1, which used the conventional technique, the highest measured voltage was 1.13p.u at the DG 4 POC after all available equipment has regulated voltage. Therefore, the proposed control scheme reduced the final voltage of 1.13p.u in scenario 1 to 1.051p.u in scenario 2. The proposed control scheme achieved this while keeping all voltage magnitudes above the minimum prescribed voltage, V_{min}, of 0.95p.u. This demonstrates the effectiveness of the newly presented algorithm in controlling voltage as compared to the conventional system. Once the control system has equalized the measured voltage magnitudes of both the OLTC and SVR with the respective calculated reference voltage. It assessed if any DG required active power reduction based on DG POC voltage magnitudes. Since there was no DG POC voltage above $V_{max} + V_{error}$ (1.06p.u), there was no requirement for DG active power reduction.

The system then moved to the final stage of power factor correction. It determined that since DGs 1-4 were dispatching 91, 6, 32, and 102% of their maximum rated reactive power capacity, respectively, to regulate voltage at t = 30 s, only DG 2 was eligible to carry out power factor correction since

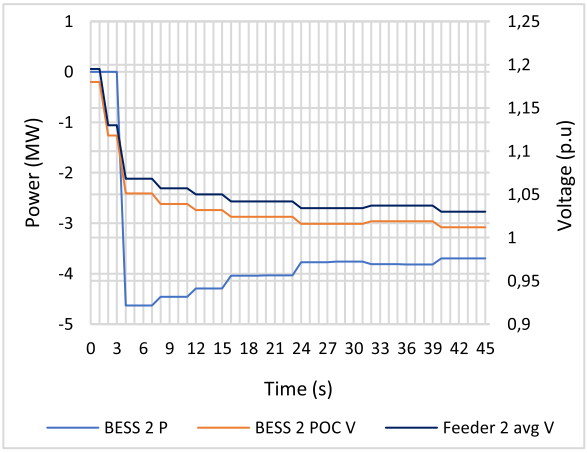

FIGURE 13. BESS 2 output power, POC voltage and feeder 2 average voltage for scenario 2.

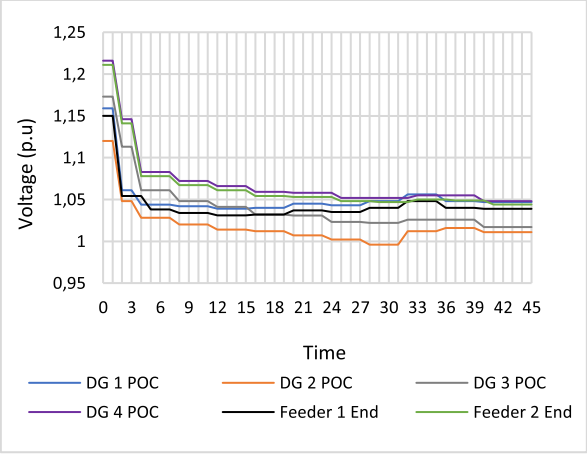

FIGURE 14. DGs POC and feeder end voltage magnitudes for scenario 2.

it is the only one importing/exporting reactive power below 30% of its maximum rated reactive power capacity. Since the reactive power measured on the substation power transformer was 5.03Mvar, leading to a power factor of 0.93 as shown at t = 30 s in Figure 11, and only one DG was eligible for power factor correction. The controller assigned DG 2 to compensate for a maximum reactive power of 5.03Mvar as depicted by Equation 19. However, due to voltage and capacity constraints, the controller only managed to get 1.42Mvar from DG 2 in accordance with Equations 19-21. Since DG 2 was already exporting 0.09Mvar for voltage regulation, it then exported 1.51Mvar in total to simultaneously control voltage and boost power factor in accordance with Equation 22. This action by DG 2 boosted the power factor from 0.93 to 0.96 as shown at t = 32s in Figure 11. When DG 2 exported a total of 1.51Mvar for controlling voltage and boosting power factor, its POC voltage increased to 1.012p.u. Since this was below 1.04p.u, based on the prescribed V_{max} of 1.05p.u, DG 2 continued performing both voltage control and boosting power factor. DG 2 will only be withdrawn

from power factor enhancement and made to focus solely on voltage regulation when its POC voltage rises above 1.04p.u, drop below 0.96p.u, or the reactive power through the substation transformer has reduced such that a power factor above 0.98 is computed when DGs are still controlling voltage through reactive power. Since the exportation of reactive power affect voltage magnitudes, the reactive power exportation by DG 2 for power factor correction at t = 32 s caused a mismatch between the measured voltage and the calculated reference voltage for both the OLTC and SVR as shown in Figures 9-10.

The SVR was at a measured voltage of 1.003p.u, with a calculated reference voltage of 0.979p.u, the OLTC was at a measured voltage of 0.990p.u, with a calculated reference voltage of 0.970p.u. The controller then changed the tap position of the SVR first, changing the measured voltage from 1.003 to 0.989p.u, which was now within 0.015p.u from its calculated reference voltage of 0.983p.u. Once the SVR voltage was within 0.015p.u from its calculated reference voltage, the controller changed the tap position of the OLTC and changed its measured voltage from 0.990 to 0.975p.u, which was now within 0.015p.u from its calculated reference voltage of 0.978p.u. At this point, the highest voltage measured within the power distribution network was 1.048p.u at the DG 4 POC, and the lowest being 0.975p.u at the OLTC location. Comparing these results to that of scenario 1 where the highest voltage ended at 1.13p.u, and the power factor at 0.78. The proposed control system succeeded in reducing the highest voltage to 1.048p.u, and the power factor improved to 0.96. This shows the effectiveness of the system presented in this paper in coordinated voltage control and power factor correction.

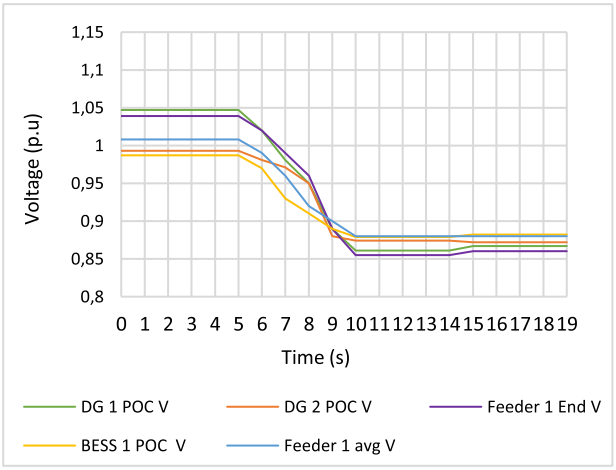

FIGURE 15. Feeder 1 voltage magnitudes without BESS 1 response.

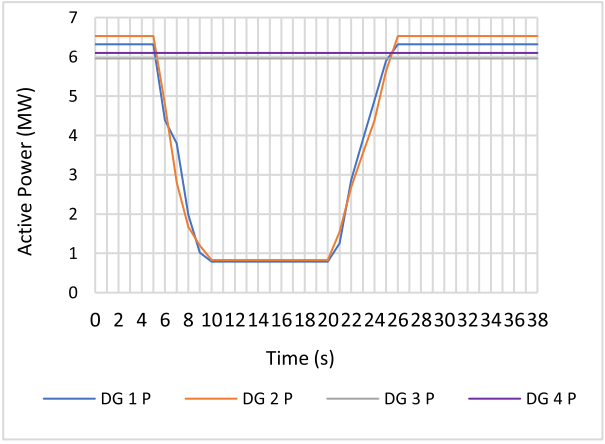

FIGURE 16. DG active power output.

C. SCENARIO 3: THE CONTROL SYSTEM'S RESPONSE TO A SUDDEN REDUCTION IN DG ACTIVE POWER OUTPUT

This scenario will demonstrate how the system uses its equipment to minimize the impact of a sudden reduction in DG active power output. This is significant as renewable DGs can produce fluctuating active power when their primary energy source is intermittent. The initial conditions of the power distribution network will be a state where the OLTC and SVR have both reached their calculated reference voltages. In addition, the active power output reduced will be that of DGs 1 and 2. The first demonstration will show how the voltage magnitudes on feeder 1 where DGs 1 and 2 are connected will behave if DG active power output is reduced while the control scheme is not fully utilized, and BESS 1 is disconnected. The network response is shown in Figure 15. The voltage magnitudes of Figure 15 are responding to the reduction in active power by DGs 1 and 2 shown in Figure 16, from t = 0 s to t = 19 s. The section from t = 20 s where the active power of DGs 1 and 2 recovers is not shown in Figure 15 since the purpose is to show how voltage magnitudes of feeder 1 respond to a DG active power output reduction when the control system is not fully utilized.

As shown in Figures 15 and 16, when the active power output of DGs 1 and 2 reduced, and BESS 1 did not respond, the voltage at the DG 1 POC, DG2 POC, feeder 1 end, and BESS 1 POC dropped to 0.861, 0.874, 0.855, and 0.879p.u, respectively. These are extremely low voltage magnitudes.The next demonstration will show how voltage magnitudes respond when the active power output of DGs 1 and 2 reduces suddenly while the proposed control scheme is fully applied with BESS 1 and 2 connected and responding accordingly. The demonstration will further evaluate how the control scheme together with its respective equipment respond when the active power of DGs 1 and 2 recovers. In addition, the demonstration will show how the proposed control scheme respond when both small and large voltage disturbances occur on the power distribution network. Therefore, on this demonstration, the control scheme is fully implemented, and the BESS is responding accordingly. The SOC for both BESS 1 and 2 was set to 50%. The results are shown in Figures 16-22.

Initially, at t = 0 s, DGs 1-4 are generating 6.32, 6.53, 5.96, and 6.1MW, respectively, as shown in Figure 16. At this

moment, the OLTC is at a measured voltage of 0.985p.u, with a calculated reference voltage of 0.977p.u, as shown in Figure 17. The SVR is at a measured voltage of 0.988p.u, with a calculated reference voltage of 0.990p.u, as shown in Figure 18. Therefore, both the OLTC and SVR are within 0.015p.u from their calculated reference voltages and the controller will not change their tap position. Furthermore, the voltage magnitudes at the DGs 1-4 POC are 1.047, 0.993, 1.023 and 1.051p.u, respectively, as shown in Figure 22. DGs 1, 3 and 4 are importing 1.36, 0.52 and 1.62Mvar of reactive power, whereas DG 2 is exporting 0.16Mvar since it is the only one with a POC voltage lower than 1p.u at 0.993p.u, as shown in Figure 19. The voltage at the end of feeders 1 and 2 is 1.039 and 1.047p.u, respectively, with the average voltage for feeders 1 and 2 at 1.008 and 1.034p.u, respectively. BESS 1 and 2 were both charging with 2.16 and 3.77MW, respectively, as shown in Figures 20-21. Therefore, in the beginning, the control system had utilized its equipment to regulate voltage magnitudes, and all measured voltage magnitudes were within acceptable range as represented at t = 0 s in Figure 22.

Then, the active power output of DGs 1 and 2 started reducing at t = 5 s as shown in Figure 16. DGs 1 and 2 moved from 6.32MW and 6.53MW to 0.79MW and 0.83MW, respectively. This caused a large voltage disturbance in feeder 1 and a small voltage disturbance in feeder 2 as shown in Figure 22. However, since the control system was fully utilized and BESS 1 responded accordingly, the voltage at the DG 1 POC, DG 2 POC, feeder 1 end, and BESS 1 POC only dropped to 0.942, 0.946, 0.940, and 0.960p.u, respectively, as shown in Figure 22. Therefore, comparing these results to that of Figure 15, where the control scheme was not fully utilized and BESS 1 disconnected, the fully implemented scheme minimized the voltage dip caused by the DGs sudden reduction of active power output by 8.1%, 7.2%, 8.5%, and 8.1% for DG 1 POC, DG 2 POC, feeder 1 end, and BESS 1 POC voltage, respectively. This is a huge improvement and shows the significance of the proposed scheme and its BESS in minimizing instantaneous voltage dips as described by the objective function of Equation 6. Therefore, when the system detected the large voltage disturbance in feeder 1 caused by the sudden reduction of active power output by DGs 1 and 2, it instructed BESS 1 to change its state from charging with 2.16MW to discharging 2.78MW, as shown at t = 5 s in Figure 20. It is this 2.78MW that BESS 1 discharged that prevented the voltage from going to levels it did when the control scheme was not fully utilized on the first demonstration of Figure 15.

Since feeder 2 only experienced a small voltage disturbance when DGs 1 and 2 reduced active power generation, the controller kept BESS 2 charging, but changed its charging power slightly from 3.77MW to 3.9MW to control the small voltage disturbance as shown in Figure 21. In addition, the controller also changed the reactive power that DG 3 is importing slightly, from 0.52Mvar to 0.65Mvar to control the small voltage disturbance in feeder 2.

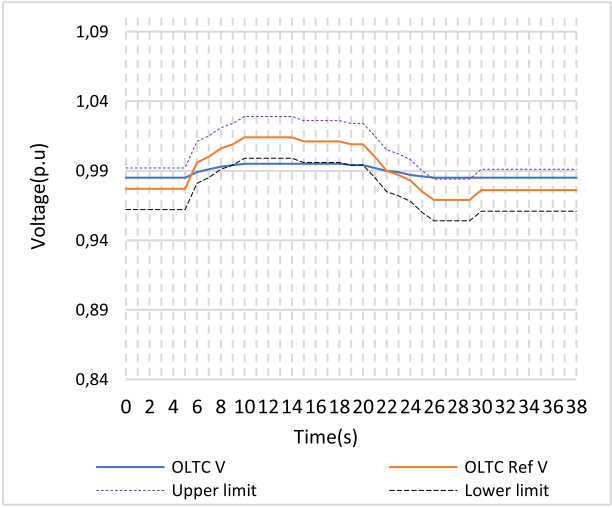

FIGURE 17. OLTC measured and calculated reference voltage.

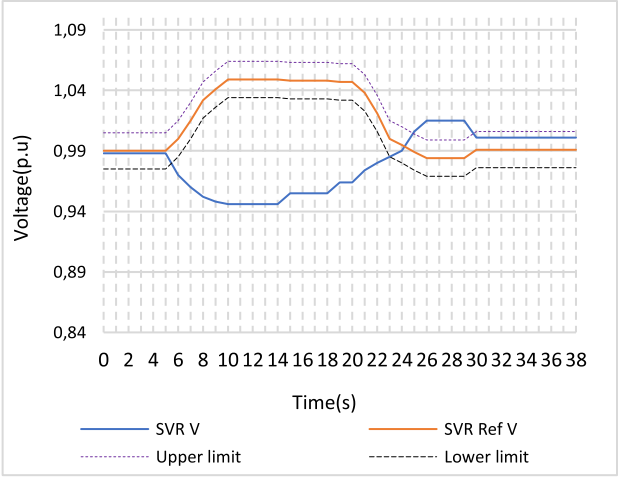

FIGURE 18. SVR measured and calculated reference voltage.

The reduction in active power output by DGs 1 and 2 at t = 5 s also caused a mismatch between the reference voltage that is calculated and the voltage that is measured for both the OLTC and SVR as shown in Figures 17-18. Therefore, after the system is done controlling BESS 1, it proceeded to the SVR, since the SVR takes precedence to the OLTC. The SVR calculated reference voltage was 1.049p.u, and the measured voltage at 0.946p.u. The SVR then altered tap position once taking the calculated SVR reference voltage and the voltage measured to 1.048 and 0.955p.u, respectively. Since they were still more than 0.015p.u apart, a second tap position change occurred taking the SVR calculated reference voltage and the voltage measured to 1.047 and 0.964p.u, respectively. Right after the SVR has changed tap position a second time, the active power generation of DGs 1 and 2 started recovering as shown at t = 20 s in Figure 16. This caused voltage magnitudes to start rising again, and hence the controller slowly changed the status of BESS 1 from discharging 2.0MW,

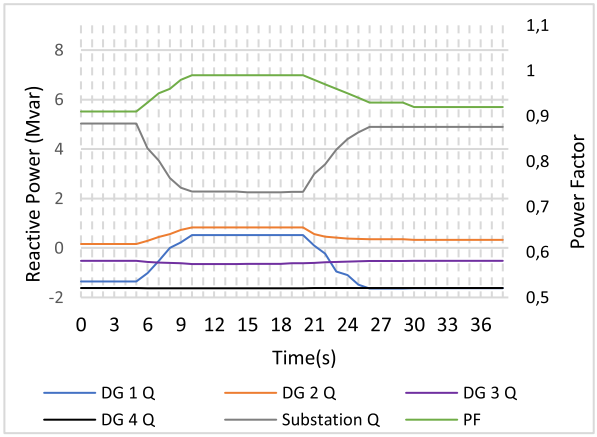

FIGURE 19. DG reactive power and the substation power factor.

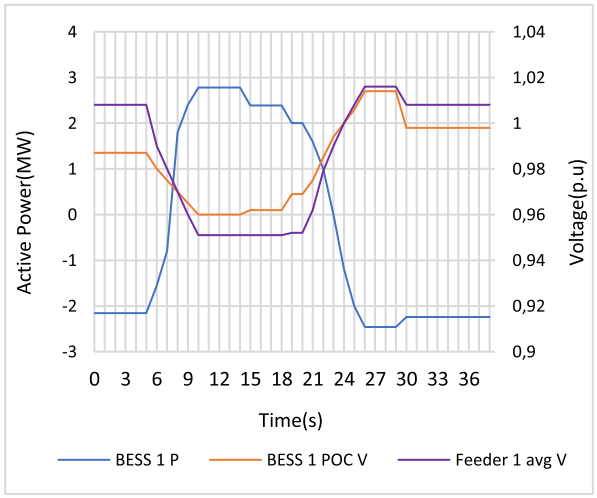

FIGURE 20. BESS 1 active power, POC and feeder 1 average voltage.

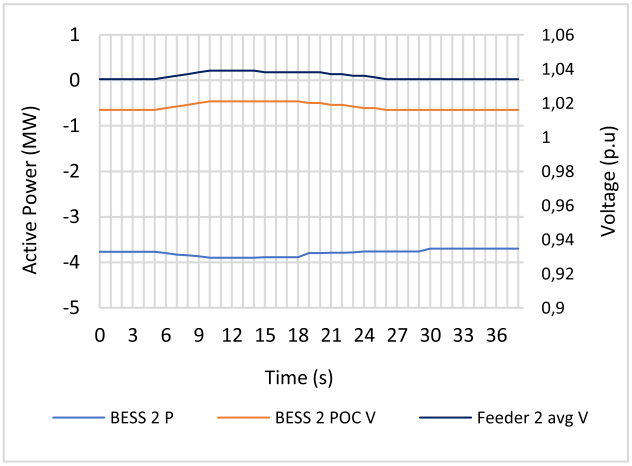

FIGURE 21. BESS 2 active power, POC and feeder 2 average voltage.

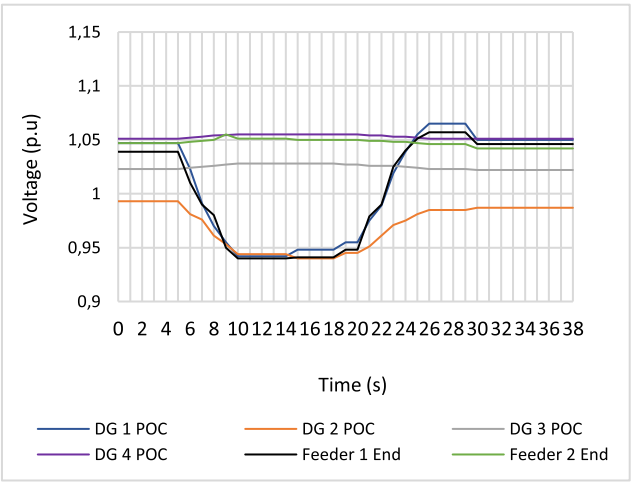

FIGURE 22. DGs and feeder end voltage magnitudes.

to charging with 2.46MW as shown in Figure 20. When the active power output of DGs 1 and 2 was fully restored at t = 27 s, there was still a mismatch between the calculated reference voltage and the voltage measured for both the OLTC and the SVR, as show in Figures 17-18. The OLTC calculated reference voltage was at 0.985p.u and its measured voltage at 0.969p.u, whereas the SVR calculated reference voltage was at 0.984p.u and the measured voltage at 1.015p.u. Since the SVR takes precedence to the OLTC, the controller changed the SVR tap position once taking the SVR measured voltage to 0.997p.u, with a calculated reference voltage of 0.991p.u. Since the SVR measured voltage was now within 0.015p.u from the calculated reference voltage, the controller turned its attention to the OLTC.

At this point, the OLTC was at a measured voltage of 0.985p.u, and the calculated reference voltage at 0.976p.u, since these were also within 0.015p.u from each other, the controller stopped instructing tap position changes for both the OLTC and SVR as shown in Figures 17-18. It can be observed that a tap change by the SVR simultaneously brought both the SVR and OLTC within 0.015p.u from their calculated reference voltages as shown at t = 30 s, in Figures 17-18. At this point, the highest measured voltage magnitude was 1.051p.u at the DG 4 POC, and the lowest voltage magnitude 0.985p.u at the OLTC location.

Scenario 3 has demonstrated the intelligent behaviour of the proposed scheme that allows it to control multiple equipment to regulate voltage, as the power system experiences large and small voltage disturbances caused by the variable active power output of renewable DGs. It can be observed that as the generation of DGs 1 and 2 drops suddenly, feeder 1 experienced a large voltage disturbance, whereas feeder 2 experienced a small voltage disturbance. However, the control system was able to continuously regulate the reactive power output of DGs, the BESS charging/discharging status, the SVR tap position, and the OLTC tap position to simultaneously control the voltage on feeder 1 experiencing a large voltage disturbance, and feeder 2 experiencing a small voltage disturbance. Furthermore, scenario 3 shows the significance of a BESS in preventing extreme voltage

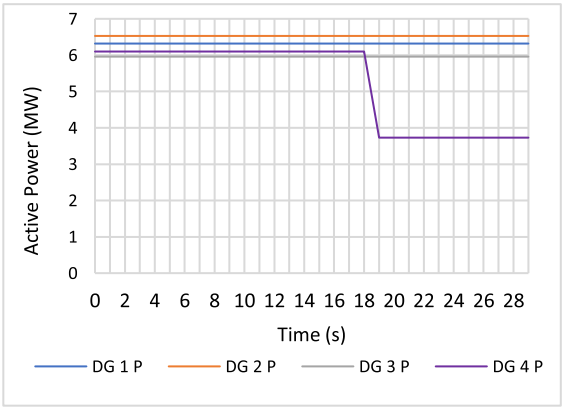

FIGURE 23. DGs active power output.

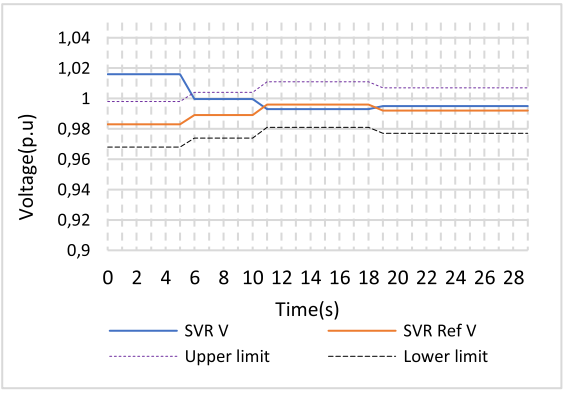

FIGURE 25. SVR measured and calculated reference voltage.

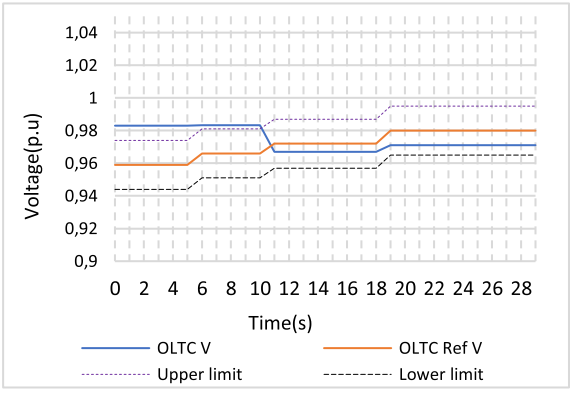

FIGURE 24. OLTC measured and calculated reference voltage.

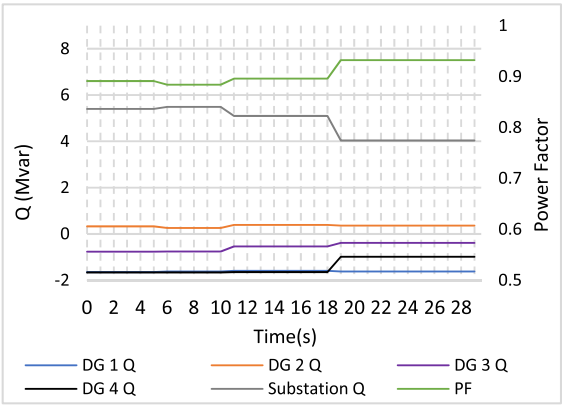

FIGURE 26. DGs reactive power and the substation power factor.

sags when DG active power output reduces suddenly. Hence, scenario 3 further confirms the ability of this multi variable control scheme in keeping voltage magnitudes within acceptable limits, and also lessen the depth of voltage dips that are caused by the erratic behaviour of renewable DGs.

D. SCENARIO 4: THE CONTROL SYSTEM'S DG ACTIVE POWER REDUCTION CAPABILITY

This scenario will illustrate the response of the control scheme when a DG POC voltage cannot be successfully brought within acceptable margin in accordance with the process of Figure 5. The initial conditions of the power system will be a state where DGs and BESS have acted, but the SVR and OLTC have not equalized their measured and calculated voltages. The network used will be that of Figure 6, however, the load on feeder 1 will remain the same at 8.43MW, and that of feeder 2 reduced to 4.62MW. Results are shown in Figures 23-29.

Initially, at t = 0 s, DGs 1-4 are generating 6.32, 6.53, 5.96, and 6.1MW, respectively, as shown in Figure 23. At this instance, the system had used DGs and BESS to regulate voltage with DGs 1, 3, and 4 importing 1.65, 0.77, and 1.66Mvar, respectively. DG 2 was exporting 0.33Mvar since its POC voltage was slightly below nominal voltage

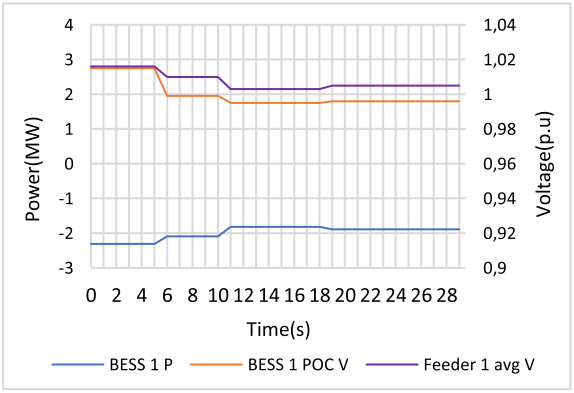

FIGURE 27. BESS 1 active power, POC and feeder 1 average voltage.

as shown in Figure 26. In addition, BESS 1 and 2 were charging at 2.31MW and 4.37MW, respectively, as shown in Figures 27 and 28. The OLTC and SVR were at a measured voltage of 0.983 and 1.016p.u, respectively, with a calculated reference voltage of 0.959 and 0.983p.u, respectively, as shown in Figures 24 and 25. Hence, both the OLTC and SVR measured voltages were not within 0.015p.u from the calculated reference voltages.

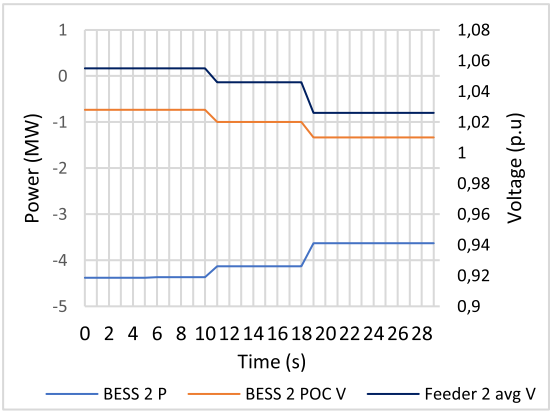

FIGURE 28. BESS 2 active power, POC and feeder 2 average voltage.

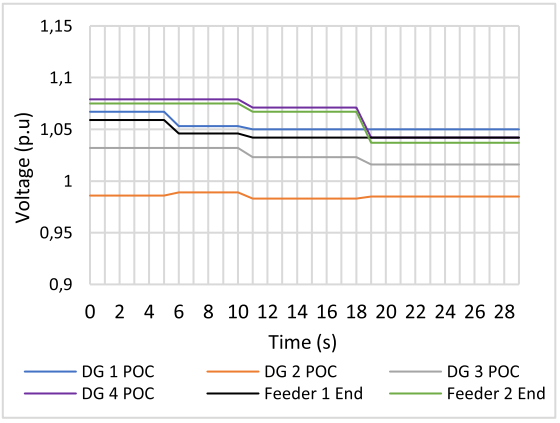

FIGURE 29. DGs and feeder end voltage magnitudes.

Therefore, the system started with the SVR and changed its tap position once taking the measured voltage to 0.999p.u, with a calculated reference voltage of 0.989p.u at t = 6 s. Since the SVR measured voltage was now 0.015p.u from the calculated reference voltage, the system moved to the OLTC and changed its tap position once as well. This changed the OLTC measured voltage to 0.967p.u, with a calculated reference voltage 0.972p.u at t = 11 s, the measured voltage was now 0.015p.u from the calculated reference voltage. At this point, the OLTC and SVR measured voltages were within 0.015p.u from the calculated reference voltages, hence, no tap position change would be carried out. Nevertheless, DGs 1-4 POC voltages were at 1.050, 0.983, 1.023 and 1.071p.u, as depicted in Figure 29 at t = 12 s. Since the system cannot change the tap positions of the OLTC and SVR, as they have reached their calculated reference voltages, and the DG 4 POC voltage is still above $(V_{max} + V_{error} = 1.06p.u)$, the control scheme then reduced the active power generation of DG 4 in accordance with Equation 17. Using the model in Matlab/Simulink, it was found that 0.56MW of active power is required to move the voltage by 0.01p.u at the DG 4 POC, this gives a sensitivity index S_p of 0.018.

Therefore, based on Equation 17, the system calculated that DG 4 must reduce its active power generation from 6.1 to 3.73MW, as shown at t = 18 s in Figure 23. The reduction of active power generation by DG 4 resulted in the DG 4 POC voltage reducing from 1.071 to 1.042p.u, as shown in Figure 29 at t = 18 s. As the voltage at the DG 4 POC dropped, the reactive power imported by DG 4 also dropped from 1.65Mvar to 0.99Mvar, as shown in Figure 26. At this point, the control scheme will only attempt to increase the active power generation of DG 4 once its POC voltage drops below 1.03p.u, this will happen when the load on feeder 2 start increasing.

Scenario 4 has illustrated the control scheme's capability to control the active power generation of DGs when the equipment dedicated to voltage regulation cannot successfully keep all voltage magnitudes within defined limits. As presented, the control scheme managed to decrease the voltage at the DG 4 POC to acceptable range by reducing the active power generation of DG 4.

VIII. CONCLUSION

In this paper, a control scheme is designed that coordinate DGs, BESS, SVR and OLTC for controlling voltage and boosting power factor in a power network with high DG generation. The design was motivated by the inefficiency of existing methods in regulating voltage when high magnitude of active power from DGs is exported to a power distribution network. When DGs are introduced to a power distribution network, especially one with long lines that have low short circuit capacity, the voltage can rise beyond acceptable limits, and the existing methods cannot successfully bring it back to acceptable range. This was demonstrated in scenario 1, where the highest voltage was 1.216p.u before the conventional method has operated, and dropped to 1.13p.u after the conventional method has operated and has reached its fixed reference voltage. In addition, the exchange of reactive power between DGs and the power system affect the power factor.

This was also confirmed in scenario 1, where the power factor was 0.99 at the beginning, and 0.78 when the conventional method has operated with DGs importing reactive power. When the newly presented control scheme that does not rely on fixed variables was implemented in scenario 2, the highest voltage was 1.216p.u at the beginning, similar to that at the beginning of scenario 1, however, the proposed technique reduced the highest voltage from 1.216 to 1.048p.u. Therefore, the proposed scheme managed to reduce voltage further by 8.20% from where the conventional method had ended. In doing so, the lowest voltage recorded was also 0.975p.u, indicating that the lower voltage limit was not breached. In addition, the power factor was 0.96 when the proposed system had operated, which is an 18.0% improvement from the conventional method. Furthermore, the proposed technique also managed to reduce the depth of a voltage dip on the average voltage of feeder 1 by 8.07%, when DG generation reduced suddenly as depicted in scenario 3. Based on the comparison between the voltage magnitudes and

power factor of the conventional method of scenario 1 and the proposed method of scenarios 2-4, it can be deduced that the proposed method is more effective in regulating voltage magnitudes and enhancing the power factor when DGs are connected.

REFERENCES

[1] U. Agarwal and N. Jain, "Distributed energy resources and supportive methodologies for their optimal planning under modern distribution network: A review," *Technol. Econ. Smart Grids Sustain. Energy*, vol. 4, no. 1, p. 3, Jan. 2019.

[2] S.-E. Razavi, E. Rahimi, M. S. Javadi, A. E. Nezhad, M. Lotfi, M. Shafie-Khah, and J. P. S. Catalžo, "Impact of distributed generation on protection and voltage regulation of distribution systems: A review," *Renew. Sustain. Energy Rev.*, vol. 105, pp. 157–167, May 2019.

[3] Z. Tang, D. J. Hill, and T. Liu, "Fast distributed reactive power control for voltage regulation in distribution networks," *IEEE Trans. Power Syst.*, vol. 34, no. 1, pp. 802–805, Jan. 2019.

[4] A. Bouakra, F. Slaoui-Hasnaoui, M. Rustom, and S. Georges, "Voltage regulation of electric power network interconnected with wind energy distributed generations," in *Proc. IEEE 2nd Int. Conf. DC Microgrids (ICDCM)*, Nuremburg, Germany, Jun. 2017, pp. 387–392.

[5] S. Repo, A. Nikander, H. Laaksonen, P. Järventausta, and P. W. Daly, "A method to increase the integration capacity of distributed generation on weak distribution networks," in *Proc. 17th Int. Conf. Electr. Distrib.*, Barcelona, Spain, May 2003, pp. 12–15.

[6] G. N. Koutroumpezis, A. S. Safigianni, G. S. Demetzos, and J. G. Kendristakis, "Investigation of the distributed generation penetration in a medium voltage power distribution network," *Int. J. Energy Res.*, vol. 34, pp. 585–593, 10 Jun. 2010.

[7] M. Chindris, A. Cziker, and A. Miron, "UPQC—The best solution to improve power quality in low voltage weak distribution networks," in *Proc. Int. Conf. Modern Power Syst. (MPS)*, Cluj-Napoca, Romania, Jun. 2017, pp. 6–9.

[8] M. G. Dozein, P. Mancarella, T. K. Saha, and R. Yan, "System strength and weak grids: Fundamentals, challenges, and mitigation strategies," in *Proc. Australas. Univ. Power Eng. Conf. (AUPEC)*, Auckland, New Zealand, Nov. 2018, pp. 27–30.

[9] R. Małkowski, M. Izdebski, and P. Miller, "Adaptive algorithm of a tap-changer controller of the power transformer supplying the radial network reducing the risk of voltage collapse," *Energies*, vol. 13, no. 20, p. 5403, Oct. 2020.

[10] A. N. Hasan and N. Tshivhase, "Voltage regulation system for OLTC in distribution power systems with high penetration level of embedded generation," *Int. Trans. Electr. Energy Syst.*, vol. 29, no. 7, Jul. 2019, Art. no. e12111.

[11] Y.-C. Jeong, E.-B. Lee, and D. Alleman, "Reducing voltage volatility with step voltage regulators: A life-cycle cost analysis of Korean solar photovoltaic distributed generation," *Energies*, vol. 12, no. 4, p. 652, Feb. 2019.

[12] M. Bazrafshan, N. Gatsis, and H. Zhu, "Optimal power flow with step-voltage regulators in multi-phase distribution networks," *IEEE Trans. Power Syst.*, vol. 34, no. 6, pp. 4228–4239, Nov. 2019.

[13] S.-B. Kim and S.-H. Song, "A hybrid reactive power control method of distributed generation to mitigate voltage rise in low-voltage grid," *Energies*, vol. 13, no. 8, p. 2078, Apr. 2020.

[14] N. Tshivhase, A. N. Hasan, and T. Shongwe, "Proposed fuzzy logic system for voltage regulation and power factor improvement in power systems with high infiltration of distributed generation," *Energies*, vol. 13, no. 16, p. 4241, Aug. 2020.

[15] N. Tshivhase, A. N. Hasan, and T. Shongwe, "A fault level-based system to control voltage and enhance power factor through an on-load tap changer and distributed generators," *IEEE Access*, vol. 9, pp. 34023–34039, Feb. 2021.

[16] I. Khan, Y. Xu, H. Sun, and V. Bhattacharjee, "Distributed optimal reactive power control of power systems," *IEEE Access*, vol. 6, pp. 7100–7111, Dec. 2018.

[17] C. Jamroen, A. Pannawan, and S. Sirisukprasert, "Battery energy storage system control for voltage regulation in microgrid with high penetration of PV generation," in *Proc. 53rd Int. Univ. Power Eng. Conf. (UPEC)*, Glasgow, U.K., Sep. 2018, pp. 4–7.

[18] T. Tewari, A. Mohapatra, and S. Anand, "Coordinated control of OLTC and energy storage for voltage regulation in distribution network with high PV penetration," *IEEE Trans. Sustain. Energy*, vol. 12, no. 1, pp. 262–272, Jan. 2021.

[19] L. Bai, T. Jiang, F. Li, H. Chen, and X. Li, "Distributed energy storage planning in soft open point based active distribution networks incorporating network reconfiguration and DG reactive power capability," *Appl. Energy*, vol. 210, pp. 1082–1091, Jan. 2018.

[20] Y. Hua, X. Shentu, Q. Xie, and Y. Ding, "Voltage/frequency deviations control via distributed battery energy storage system considering state of charge," *Appl. Sci.*, vol. 9, no. 6, p. 1148, Mar. 2019.

[21] J. Tan and Y. Zhang, "Coordinated control strategy of a battery energy storage system to support a wind power plant providing multi-timescale frequency ancillary services," *IEEE Trans. Sustain. Energy*, vol. 8, no. 3, pp. 1140–1153, Jul. 2017.

[22] M. Zeraati, M. E. H. Golshan, and J. M. Guerrero, "Distributed control of battery energy storage systems for voltage regulation in distribution networks with high PV penetration," *IEEE Trans. Smart Grid*, vol. 9, no. 4, pp. 3582–3593, Dec. 2016.

[23] K. Kotsalos, I. Miranda, J. L. Dominguez-Garcia, H. Leite, N. Silva, and N. Hatziargyriou, "Exploiting OLTC and BESS operation coordinated with active network management in LV networks," *Sustainability*, vol. 12, no. 8, p. 3332, Apr. 2020.

[24] X. Liu, A. Aichhorn, L. Liu, and H. Li, "Coordinated control of distributed energy storage system with tap changer transformers for voltage rise mitigation under high photovoltaic penetration," *IEEE Trans. Smart Grid.*, vol. 3, no. 2, pp. 897–906, Jun. 2012.

[25] M. Chamana and B. H. Chowdhury, "Optimal voltage regulation of distribution networks with cascaded voltage regulators in the presence of high PV penetration," *IEEE Trans. Sustain. Energy*, vol. 9, no. 3, pp. 1427–1436, Jul. 2018.

[26] M. Aryanezhad, "Management and coordination of LTC, SVR, shunt capacitor and energy storage with high PV penetration in power distribution system for voltage regulation and power loss minimization," *Int. J. Elect. Power Energy Syst.*, vol. 100, pp. 178–192, Sep. 2018.

[27] M. Zeraati, M. E. H. Golshan, and J. M. Guerrero, "A consensus-based cooperative control of PEV battery and PV active power curtailment for voltage regulation in distribution networks," *IEEE Trans. Smart Grid*, vol. 10, no. 1, pp. 670–680, Jan. 2019.

[28] J. Faiz and B. Siahkolah, "Differences between conventional and electronic tap-changers and modifications of controller," *IEEE Trans. Power Del.*, vol. 21, no. 3, pp. 1342–1349, Jun. 2006.

[29] C. R. Sarimuthu, V. K. Ramachandaramurthy, K. R. Agileswari, and H. Mokhlis, "A review on voltage control methods using on-load tap changer transformers for networks with renewable energy sources," *Renew. Sustain. Energy Rev.*, vol. 62, pp. 1154–1161, Sep. 2016.

[30] F. A. Viawan, A. Sannino, and J. Daalder, "Voltage control with on-load tap changers in medium voltage feeders in presence of distributed generation," *Electr. Power Syst. Res.*, vol. 77, pp. 1314–1322, Aug. 2007.

[31] F. Bai, R. Yan, T. K. Saha, and D. Eghbal, "A new remote tap position estimation approach for open-delta step-voltage regulator in a photovoltaic integrated distribution network," *IEEE Trans. Power Syst.*, vol. 33, no. 4, pp. 4433–4443, Jul. 2018.

[32] C. Deckmyn, T. L. Vandoorn, B. Meersman, L. Gevaert, L. Vandevelde, and J. Desmet, "A coordinated voltage control strategy for on-load tap changing transformers with the utilisation of distributed generators," in *Proc. IEEE Int. Energy Conf. (ENERGYCON)*, Leuven, Belgium, Apr. 2016, pp. 4–8.

[33] M. A. Azzouz and E. F. El-Saadany, "Optimal coordinated volt/VAR control in active distribution networks," in *Proc. IEEE PES Gen. Meeting Conf. Expo.*, National Harbor, MD, USA, Jul. 2014, pp. 27–31.

[34] A. Mazza, H. Mirtaheri, G. Chicco, A. Russo, and M. Fantino, "Location and sizing of battery energy storage units in low voltage distribution networks," *Energies*, vol. 13, no. 1, p. 52, Dec. 2019.

[35] S. Lotsu, Y. Yoshida, K. Fukuda, and B. He, "Effectiveness of a power factor correction policy in improving the energy efficiency of large-scale electricity users in Ghana," *Energies*, vol. 12, no. 13, p. 2582, Jul. 2019.

[36] L. Huang, J. Xu, Y. Sun, M. Chen, and H. Xu, "Voltage stability analysis and monitoring based on short circuit capacity," in *Proc. IEEE Int. Conf. Power Syst. Technol. (POWERCON)*, Auckland, New Zealand, Oct. 2012, pp. 1–5.

[37] A. D. Pizzc, L. Di Noia, D. Lauria, M. Crispino, A. Cantiello, and F. Mottola, "Control of OLTC distribution transformer addressing voltage regulation and lifetime preservation," in *Proc. Int. Symp. Power Electron., Electr. Drives, Automat. Motion (SPEEDAM)*, Amalfi, Italy, Jun. 2018, pp. 20–22.
[38] M. Sedghi, A. Ahmadian, and M. Aliakbar-Golkar, "Optimal storage planning in active distribution network considering uncertainty of wind power distributed generation," *IEEE Trans. Power Syst.*, vol. 31, no. 1, pp. 304–316, Jan. 2016.
[39] K. C. Divya and J. Østergaard, "Battery energy storage technology for power systems—An overview," *Electr. Power Syst. Res.*, vol. 79, no. 4, pp. 511–520, Apr. 2009.
[40] M. Beaudin, H. Zareipour, A. Schellenberg, and W. Rosehart, "Energy storage for mitigating the variability of renewable electricity sources," *Energy Storage for Smart Grids, Planning and Operation for Renewable and Variable Energy Resources*. Amsterdam, The Netherlands: Elsevier, 2015, pp. 1–33.
[41] T. Mchunu, "Grid connection code for renewable power plants (RPPs) connected to the electricity transmission system (TS) or the distribution system (DS) in South Africa, version 3.0," Nat. Energy Regulator South Africa, Pretoria, South Africa, Tech. Rep., Sep. 2020.

NDAMULELO TSHIVHASE received the B.Eng. degree in electrical and electronic engineering and the M.Eng. degree in electrical engineering from the University of Johannesburg, South Africa, in 2013 and 2019, respectively. He is currently a power system engineer focused on the integration of renewable power plants into the power systems.

ALI N. HASAN received the B.Eng. degree in electrical and electronic engineering from Hashemite University, Jordan, in 2005, the M.Eng. degree in electrical engineering from North West University, South Africa, in 2010, and the D.Ing. (Ph.D.) degree in electrical and electronic engineering from the University of Johannesburg, South Africa, in 2014. He was a Senior Lecturer with the Department of Electrical and Electronic Engineering Technology, University of Johannesburg, South Africa. He is currently an Assistant Professor with the Higher Colleges of Technology, Abu Dhabi. His research work focuses on the applications of artificial intelligence in energy, power, and communication systems.

THOKOZANI SHONGWE (Member, IEEE) received the B.Eng. degree in electronic engineering from the University of Swaziland, Swaziland, in 2004, the M.Eng. degree in telecommunications engineering from the University of the Witwatersrand, South Africa, in 2006, and the D.Eng. degree from the University of Johannesburg, South Africa, in 2014. He is currently an Associate Professor with the Department of Electrical and Electronic Engineering Technology, University of Johannesburg. His research fields are in digital communications and error correcting coding. His research interests include power-line communications, cognitive radio, smart grid, visible light communications, machine learning, and artificial intelligence. He was a recipient of the 2014 University of Johannesburg Global Excellence Stature (GES) Award, which was awarded to him to carry out his postdoctoral research with the University of Johannesburg. In 2016, he was a recipient of the TWAS-DFG Cooperation Visits Program funding to do research in Germany. He received the Post-Graduate Merit Award Scholarship to pursue his master's degree with the University of the Witwatersrand, in 2005, which is awarded on a merit basis. In 2012, he (and his coauthors) received an Award of the Best Student Paper at the IEEE ISPLC 2012 (power line communications conference), Beijing, China.